

AD-757612

EDGEWOOD  
ARSENAL

AD

**EDGEWOOD ARSENAL  
TECHNICAL REPORT**

**EATR 4696**



**THERMOCOUPLE MEASUREMENT OF HEAT FLUX  
AND APPLICATION TO IGNITION OF WOOD**

by

C. Stuart Kelley, Ph. D.  
Aldean Bengé

Chemical Laboratory

March 1973



**DEPARTMENT OF THE ARMY  
Headquarters, Edgewood Arsenal  
Aberdeen Proving Ground, Maryland 21010**

Approved for public release; distribution unlimited.

Disclaimer

The findings in this report are not to be construed as an official Department of the Army position unless so designated by other authorized documents.

The use of trade names in this report does not constitute an official endorsement or approval of the use of such commercial hardware or software. This report may not be cited for purposes of advertisement.

Disposition

Destroy this report when no longer needed. Do not return it to the originator.

EDGEWOOD ARSENAL TECHNICAL REPORT

EATR 4696

THERMOCOUPLE MEASUREMENT OF HEAT FLUX  
AND APPLICATION TO IGNITION OF WOOD

by

C. Stuart Kelley, Ph. D.  
Aldean Bengé

Physical Research Division  
Chemical Laboratory

March 1973

Approved for public release; distribution unlimited.

Project 1W562603A065

DEPARTMENT OF THE ARMY  
Headquarters, Edgewood Arsenal  
Aberdeen Proving Ground, Maryland 21010

## FOREWORD

The work described in this report was authorized under Project 1W562603A065, Flame, Incendiary, and Smoke Technology. The work was started in June 1971 and completed in August 1971.

Reproduction of this document in whole or in part is prohibited except with permission of the Commander, Edgewood Arsenal, Attn: SMUEA-TS-R, Aberdeen Proving Ground, Maryland 21010; however, DDC and the National Technical Information Service are authorized to reproduce the document for United States Government purposes.

## Acknowledgments

The authors wish to express their gratitude to Mr. Thomas G. Lancaster for performing the temperature versus time and angle experiments.

## DIGEST

Measurements reported here on flames from thickened hydrocarbons indicate that close to, but outside, the flame outline the thermocouple temperature can be converted to the heat flux emitted by the flame. From the thermocouple data, the dependence of the time to ignition for a wood target outside the flame on the angle from the flame symmetry axis is established. For angles less than about 10 degrees, the ignition time is relatively constant; for larger angles, it increases rapidly. The dependence of the time to ignition on the height above the flame agent is also established; it increases rapidly with increasing height. Measurements reported here on the ignition of wood confirm the predicted dependence of the ignition time on the time-dependent incident heat flux intensity.

BLANK

## CONTENTS

	<u>Page</u>
I. INTRODUCTION . . . . .	7
II. EXPERIMENTAL PROCEDURES AND RESULTS . . . . .	7
III. DATA ANALYSIS . . . . .	10
IV. THEORY . . . . .	15
V. APPLICATIONS . . . . .	20
VI. CONCLUSIONS . . . . .	25
LITERATURE CITED . . . . .	27
APPENDIX, Presentation of Results of Experiments Designed to Investigate the Validity of Equation (5) . . . . .	29
DISTRIBUTION LIST . . . . .	41

## LIST OF FIGURES

### Figures

1	Experimental Setup . . . . .	8
2	Thermocouple Temperature Versus Time for Thermocouple at $r = 40$ cm and Specific Values of $\phi$ . . . . .	9
3	Normalized Thermocouple Temperature Versus $\phi$ . . . . .	10
4	Dependences of Normalized Temperature and Heat Flux on $\phi$ . . . . .	11
5	Dependences of Temperature Fraction and Heat Flux Fraction on $\phi$ . . . . .	14
6	Dependences of Temperature Fraction and Average Heat Flux Fraction on $\phi$ . . . . .	14
7	Coordinates of Interest for a Thermocouple Bead . . . . .	15
8	Theoretical Thermocouple Temperature Versus Incident Radiant Heat Flux . . . . .	18
9	Dependence of Hypothetical Ignition Time on $\phi$ . . . . .	21

# LIST OF FIGURES (Contd)

<u>Figures</u>		<u>Page</u>
10	Dependence of Thermocouple Temperature T on Time t at Various Heights above the Flame Agent . . . . .	22
11	Dependence of Thermocouple Temperature T on Height z above the Flame Agent at Various Times During the Burning of the Agent . . . . .	23
12	Dependence of Hypothetical Ignition Time $t'_{ig}$ on Height z Above the Flame Agent . . . . .	24
Table	Comparison of Equation (3) with Experimentally Determined Heat Flux Values . . . . .	19

# THERMOCOUPLE MEASUREMENT OF HEAT FLUX AND APPLICATION TO IGNITION OF WOOD

## I. INTRODUCTION.

A burning flame agent generates heat which is emitted by both the flame and the flame agent. The heat emitted by the flame, primarily radiative and convective, is directed upward and outward. On the other hand, the heat emitted by the flame agent, primarily conductive, is directed downward to the agent substrate.

Most studies of the two components have been concerned with the dependence of the thermocouple temperature on time for various positions of the thermocouple about the flame.<sup>1-3</sup> With the increased availability of a variety of commercial heat flux meters, measurements of the radiative and convective heat flux emitted by flames have been performed.<sup>4</sup> Also, for specific flame agents, the distribution of this heat flux has been determined.<sup>5</sup> For hydrocarbon-based flame agents, the fraction of the heat which is conductive has been reported to be small.<sup>4</sup>

The time to ignition of a cellulosic solid exposed to a constant radiative heat flux has been determined<sup>6</sup> and has been extended to include the effects of time-dependent heat fluxes.<sup>7</sup> This ignition criterion has been used to predict the dependence of the time to ignition of wood within a flame on both the height of the wood above the flame agent and the mass of the flame agent.<sup>7</sup>

This report concerns the relation between thermocouple temperature measurements and heat flux measurements (about a burning flame agent) and the application of thermocouple temperature versus time data to the determination of target ignition times for cellulosic solids.

## II. EXPERIMENTAL PROCEDURE AND RESULTS.

In each test, 25 grams of 2% M4 thickened unleaded gasoline was placed in a stainless steel cup of 6.5 cm inner diameter, 7.1 cm outer diameter, 2.2 cm inner height, and 2.5 cm outer height. Samples were ignited and allowed to burn to completion. The cup rested on a transite board which formed the base of the laboratory hood. A fan located in the ceiling of the hood

---

<sup>1</sup> Wilkes, G. B. NDRC Contract. Final Report. Symbol No. 574. Radiation Characteristics of Burning Incendiary Materials. June 1942. UNCLASSIFIED Report.

<sup>2</sup> Koch, H.W. Vergleichsmessungen von Temperature und Wärmestromdichten an Brandstoffen. Technische Mitteilung ISL-T 40/67, Deutsch-Französisches Forschungsinstitut Saint-Louis 10, 11 (1967).

<sup>3</sup> Kelley, C. S. EATR 4436. The Use of Spatially-Separated Series-Linked Thermocouples in Flame Evaluation. August 1970. UNCLASSIFIED Report.

<sup>4</sup> Brown, R. E., Garfinkle, D. R., and Andersen, W. H. Shock Hydrodynamics, Inc. Final Report SH11-6245-3. Contract DAAA-15-69-C-0301. Evaluation Techniques for Flame and Incendiary Agents. June 1970. UNCLASSIFIED Report.

<sup>5</sup> Kelley, C. S. EATR 4492. Dependence of Heat Flux (Radiative Plus Convective) From Burning Flame Agents on the Angle from the Flame Symmetry Axis. February 1971. UNCLASSIFIED Report.

<sup>6</sup> Welker, J. R., and Sliepcevich, C. M. Final Report, Contract DAAA-15-67-C-0074. Susceptibility of Potential Target Components to Defeat by Thermal Action (U). July 1970. UNCLASSIFIED Report.

<sup>7</sup> Kelley, C. S. EATR 4539. Piloted Ignition Times for Cellulosic Solids Exposed to Time-Dependent Heat Fluxes. August 1971. UNCLASSIFIED Report.

exhausted combustion products at a constant velocity somewhat larger than the velocity due to the buoyancy effects. Each porcelain-sheathed Chromel-Alumel thermocouple with the bead exposed was placed at the desired angle  $\phi$  and at a radius of 40 cm from the center of the pool base (figure 1).

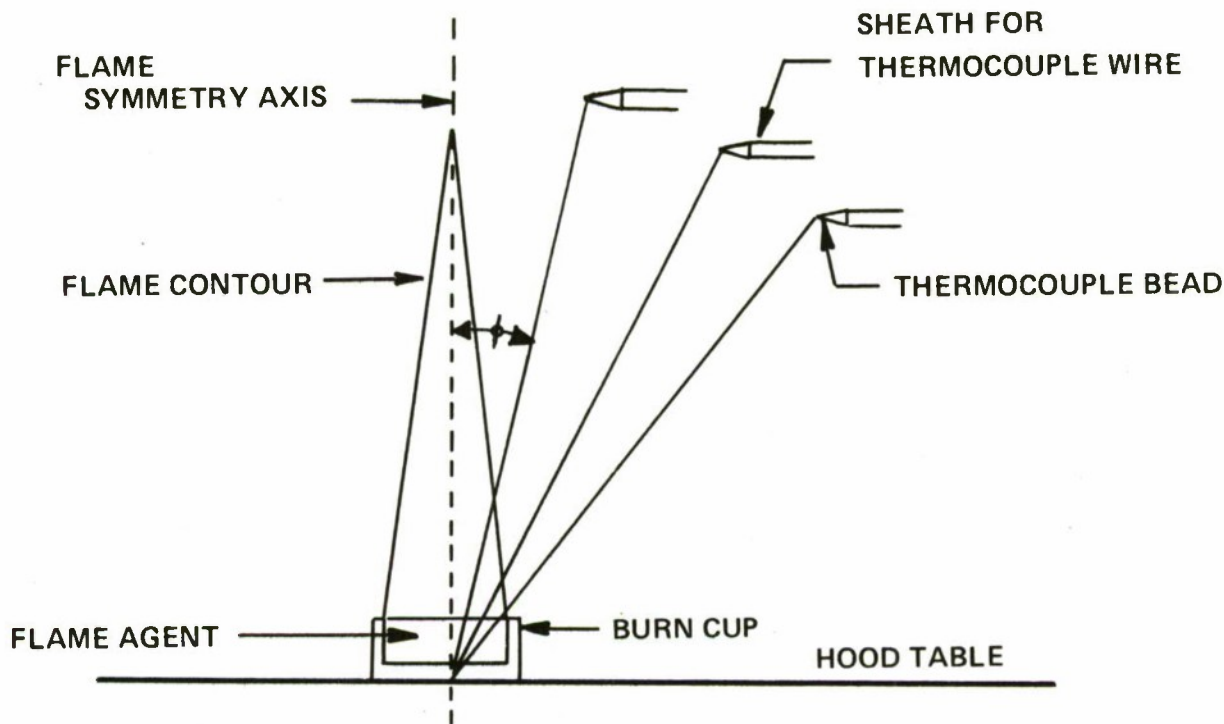


Figure 1. Experimental Setup

Three series of tests were conducted. In Test Series A, the thermocouples were placed at  $\phi = 15^\circ$ ,  $\phi = 20^\circ$ ,  $\phi = 25^\circ$ , and  $\phi = 40^\circ$ . The thermocouples in Test Series B were placed at  $\phi = 10^\circ$ ,  $\phi = 30^\circ$ , and  $\phi = 50^\circ$ . In Test Series C, the thermocouples were placed at  $\phi = 0^\circ$  and  $\phi = 5^\circ$ . In each test series, 10 identical experiments were conducted in order to reduce the scatter in the data. The electromotive force (emf) of each thermocouple was recorded for the duration of burning by a Model 1108 Honeywell Multichannel Visicorder, which produced a strip recording of the emf versus time of each thermocouple. All reference junctions were maintained at  $25^\circ\text{C}$ .

For each test series, the average temperature as a function of time was obtained for each angle  $\phi$ . From the strip recording, emf values were taken at intervals corresponding to every 20 seconds. At each interval and at each value of  $\phi$ , the 10 emf values were averaged and converted to temperature. Thus, the average thermocouple temperature was obtained at 20-second intervals throughout the duration of burning and for each value of  $\phi$ . The average temperature at each value

of  $\phi$  was then plotted as a function of time (displayed in figure 2). From figure 2 it can be seen that the peak temperature is reached about one-third through the burn duration.

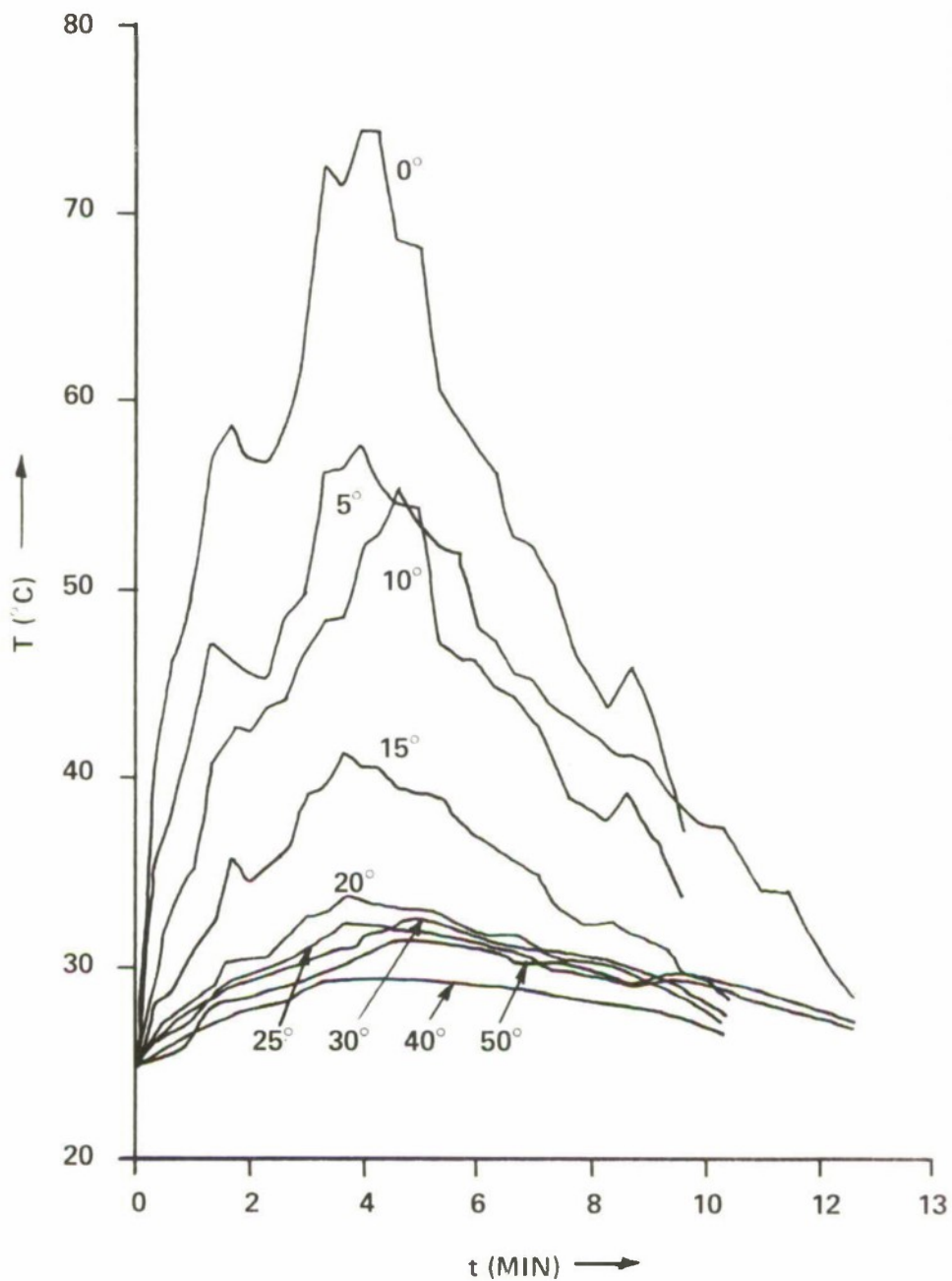


Figure 2. Thermocouple Temperature Versus Time for Thermocouple at  $r = 40$  cm and Specific Values of  $\phi$

### III. DATA ANALYSIS.

From the experimental data presented in figure 2, the dependence of the thermocouple temperature on the angle  $\phi$  was determined. The procedure used to obtain this dependence will now be described.

The curves in figure 2 were first reduced to plots of the temperature above ambient ( $25^{\circ}\text{C}$ ) versus time for each of the nine values of  $\phi$ . Then, the value of  $T - 25$  at one instant in time,  $t_0$ , was found for each value of  $\phi$ . Then a plot of  $T - 25$  versus  $\phi$  was made for each of eight values of  $t_0$  ( $t_0 = 1, 2, \dots, 8$  min). Each of the eight plots was then normalized by choosing its value of  $T(t_0) - 25$  at  $\phi = 0^{\circ}$  to be unity. This normalized temperature may be written as

$$T_N(t_0) = [T(\phi, t_0) - 25] [T(\phi = 0, t_0) - 25]^{-1}$$

The eight graphs of  $T_N(t_0)$  versus  $\phi$  were superposed, and the average over  $t_0$  of the  $T_N(\phi, t_0)$  was found. This average,  $T_N(\phi)$ , is plotted versus  $\phi$  in figure 3. The dependence is characterized by a rapid decrease in  $T_N$  with increasing  $\phi$  to  $20^{\circ}$  and then by a less rapid decrease above  $20^{\circ}$ . A suggested curve is superposed on the data points in figure 3.

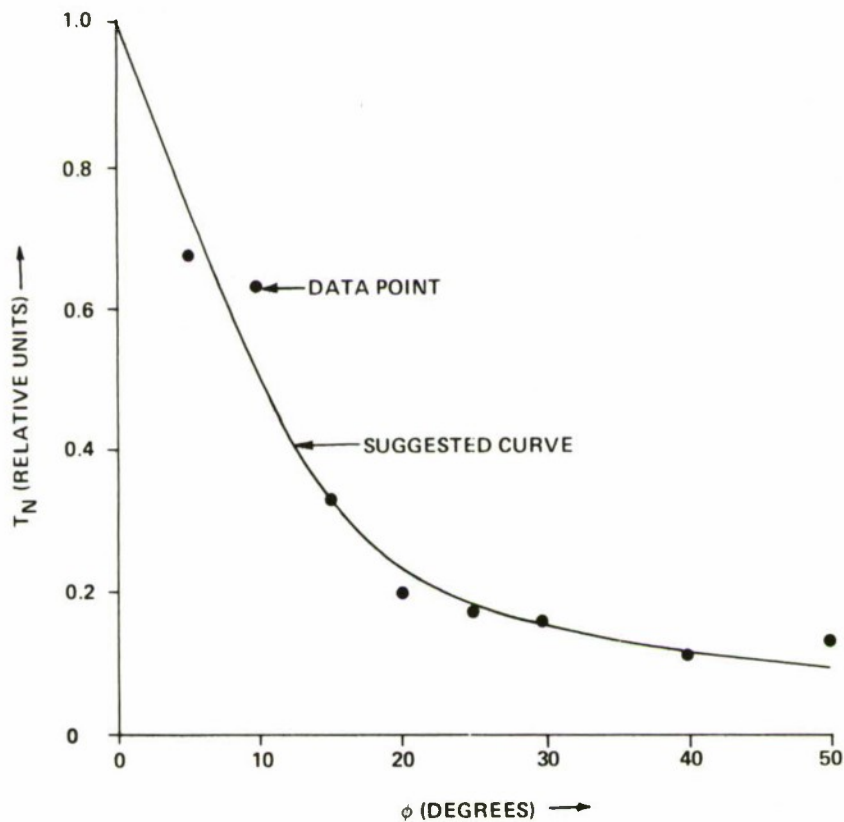


Figure 3. Normalized Thermocouple Temperature Versus  $\phi$

In figure 4, the suggested curve of figure 3 is superposed on similar plots (also for  $r = 40$  cm), obtained by Kelley.<sup>5</sup> These latter curves, however, are derived from heat flux measurements performed on 2% M4 thickened Napalm Test Solvent (NTS) and on Westco gel. The NTS is composed of 57% heptane, 20% cyclohexane, 18% benzene, 5% 2,2,4-trimethyl pentane; Westco gel is described elsewhere.<sup>8</sup> For these two fuels, the ordinate of figure 4 is the normalized heat flux,  $S_N$ , rather than  $T_N$ .

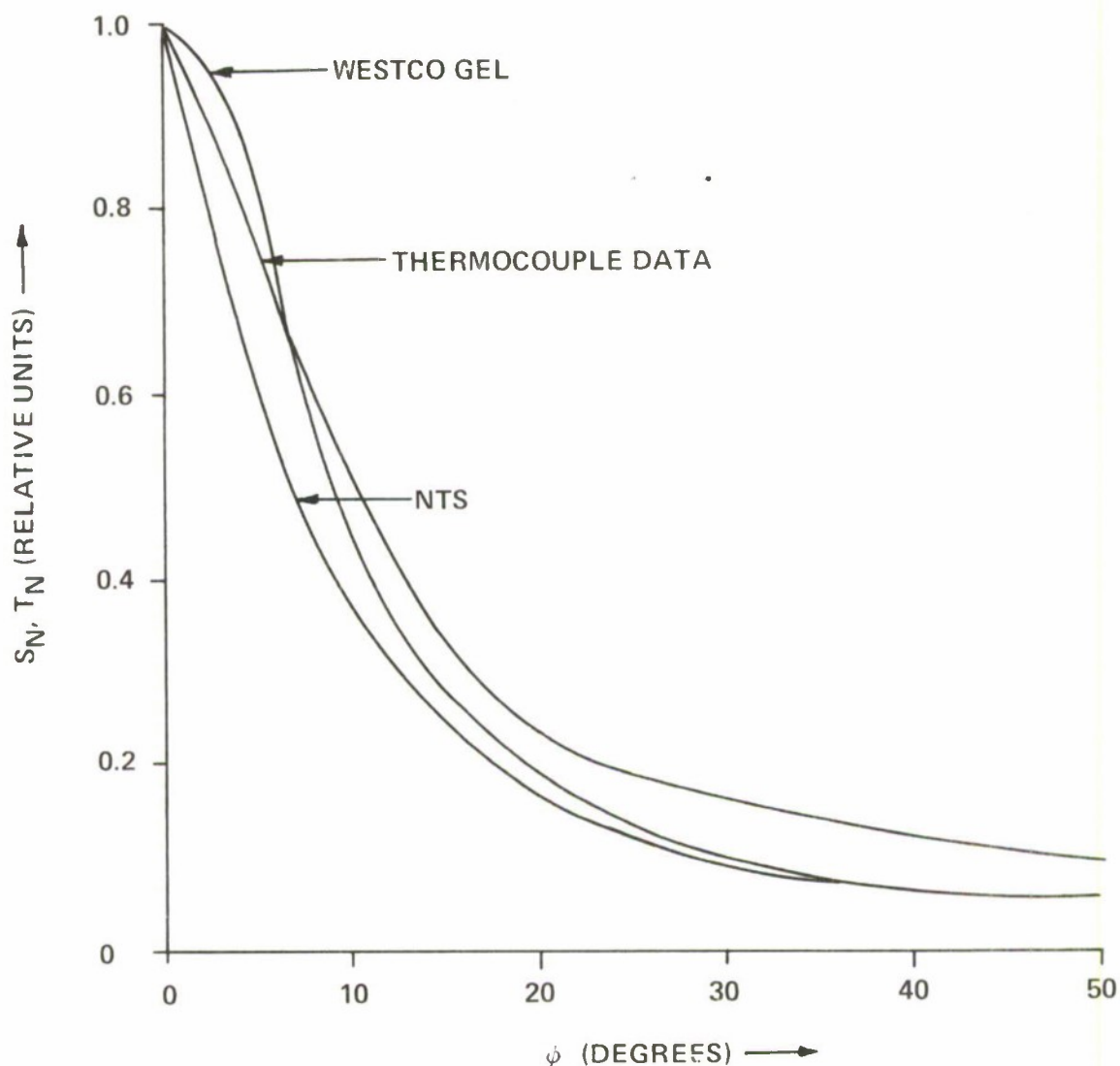


Figure 4. Dependences of Normalized Temperature and Heat Flux on  $\phi$

<sup>8</sup> Technical Documentary Report No. ATL-TDR-64-34, Instantaneous Preparation of Flame Fuels for Fire Bombs, Prepared Under Contract No. AF 08 (635)-3638, AFSC Project 670A, by Westco Research, a Division of The Western Company of North America, January 1964. CONFIDENTIAL Report.

It can be seen from figure 4 that the basic dependences of  $S_N$  and  $T_N$  on  $\phi$  are the same: a rapid drop for small values of  $\phi$  and then a levelling off. Up to  $\phi = 10^\circ$ , the dependences of  $S_N$  and  $T_N$  are the same to within about 20%, and, in general, the smaller the  $\phi$  the closer the agreement. It is important to note that  $S_N$  and  $T_N$  were obtained from different flame agents as well as from different pool diameters (6.5 cm for  $T_N$  and 7.6 cm for  $S_N$ ). Because the flame-height to pool-diameter ratio changes with pool diameter, the dependences of  $S_N$  and  $T_N$  would not be expected to coincide precisely.

From the suggested curve in figure 3, the quantity

$$\phi_n = 2.5n^\circ$$

$$A_T(\phi_n) = \int_0^{\phi_n} T_N \sin \phi d\phi$$

was determined for  $n = 0, 1, 2, \dots, 20$ . The upper limit of  $50^\circ$  occurred because the experimental data did not span  $\phi > 50^\circ$ . The quantity  $A_T(\phi_n)$  represents the sum of the temperature rise within an inverted cone of half-angle  $\phi_n$ , whose apex is located at the center of the base of the flame agent. The quantity

$$A_S(\phi_n) = \int_0^{\phi_n} S_N \sin \phi d\phi$$

represents the heat flux emitted within a similar inverted cone. The fraction  $f_s$  of the total heat flux (i.e.,  $\phi_n = 50^\circ$ ) which is contained in such a cone is

$$f_s = A_S(\phi_n)/A_S(50^\circ) = \frac{\int_0^{\phi_n} S_N \sin \phi d\phi}{\int_0^{50^\circ} S_N \sin \phi d\phi}$$

The fraction

$$f_T = A_T(\phi_n)/A_T(50^\circ) = \frac{\int_0^{\phi_n = 2.5^\circ} T_N \sin \phi d\phi}{\int_0^{50^\circ} T_N \sin \phi d\phi}$$

was computed at  $2.5^\circ$  intervals over  $0 \leq \phi \leq 50^\circ$ . The resulting values of  $f_T$  as functions of  $\phi$  are shown in figure 5. Figure 5 also includes the dependences of  $f_s$  on  $\phi$  for 7.6-cm-diameter pools of burning NTS and Westco gel. The dots representing the M4 thickened unleaded gasoline in figure 5 lie below the curves for Westco gel and NTS. This is consistent with figure 4, since a larger portion of the energy is emitted at larger angles for M4 thickened unleaded gasoline than is emitted for the other two flame agents. However, the basic dependences of  $f_s$  and  $f_T$  are similar and agree to within about 20%.

As may be seen from figure 5, all three dependences are similar; the data points lie near the curve for NTS, and somewhat further from the curve for Westco gel. This indicates that the dependence of thermocouple temperature (above ambient) on  $\phi$  parallels that of the heat flux, suggesting that the thermocouple temperature may be scaled to the heat flux for points close to, but outside, the flame.

Figure 6 shows  $f_T$  compared to  $f_s$  (here  $f_s$  is the average of the  $f_s$  for NTS and Westco gel) over the entire range of  $f_s$ . Since  $f_T$  just spanned the range  $0 \leq \phi \leq 50^\circ$ , the value of  $f_T$  at  $\phi=50^\circ$  was chosen to coincide with  $f_s$  at  $\phi = 50^\circ$ . The close correspondence between  $f_s$  and  $f_T$  is shown in figure 6.

Taking the  $T(\phi = 0, t)$  curve in figure 2 and choosing its maximum temperature ( $49.3^\circ$  above ambient) to coincide with the heat flux ( $0.201 \text{ cal-cm}^{-2}\text{-sec}^{-1}$ ) at a corresponding position for Westco gel, the scale factor to convert thermocouple temperature (above ambient) to heat flux (also above ambient) is  $4.07 \times 10^{-3} \text{ cal-cm}^{-2}\text{-sec}^{-1}\text{-(}^\circ\text{C)}^{-1}$ . Because the three curves of figure 4 do not coincide exactly, this scale factor must be regarded as an approximation. To check its accuracy,

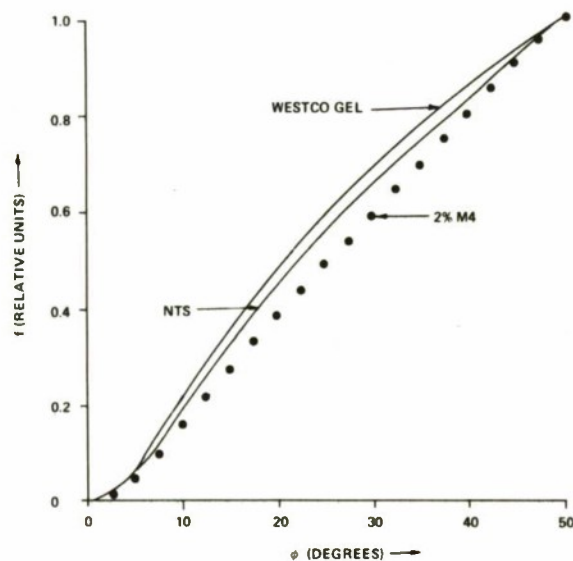


Figure 5. Dependences of Temperature Fraction and Heat Flux Fraction on  $\phi$

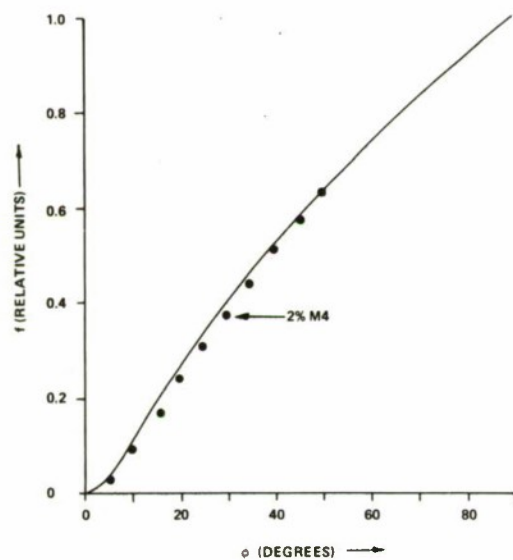


Figure 6. Dependences of Temperature Fraction and Average Heat Flux Fraction on  $\phi$

scale factors were computed for  $\phi = 20^\circ$  and  $\phi = 40^\circ$ . They are  $4.00 \times 10^{-3} \text{ cal-cm}^{-2}\text{-sec}^{-1}\text{-(}^\circ\text{C)}^{-1}$  and  $3.07 \times 10^{-3} \text{ cal-cm}^{-2}\text{-sec}^{-1}\text{-(}^\circ\text{C)}^{-1}$ , respectively. An average value for the scale factor may be taken as

$$4 \times 10^{-3} \text{ cal-cm}^{-2}\text{-sec}^{-1}\text{-(}^\circ\text{C)}^{-1} \quad (1)$$

which appears to be accurate to within 25%. It is to be emphasized that this empirical scale factor was arrived at for measurements taken at  $r = 40 \text{ cm}$  and  $0 \leq \phi \leq 50^\circ$ .

#### IV. THEORY.

This section is devoted to the relation between the radiative heat flux  $S$  incident on a thermocouple and the temperature  $T$  of the thermocouple. For simplicity, heat losses by conduction through the thermocouple wires are neglected, although these can be considerable in practice. The heat transferred between the thermocouple and the source of the radiation are restricted to graybody absorption and emission processes. That is, the thermocouple bead is characterized by an average absorption coefficient  $\alpha$ , and an average emissivity  $\epsilon$ . These values of  $\alpha$  and  $\epsilon$  shall represent averages over that range of wavelength for which the incident radiation (taken as wavelength - independent over this range) is non-zero.

Let the thermocouple bead be a sphere of radius  $a$ , centered at the origin of the spherical coordinate system (figure 7). The non-diverging radiative flux is incident on the sphere and is parallel to the  $z$ -axis.

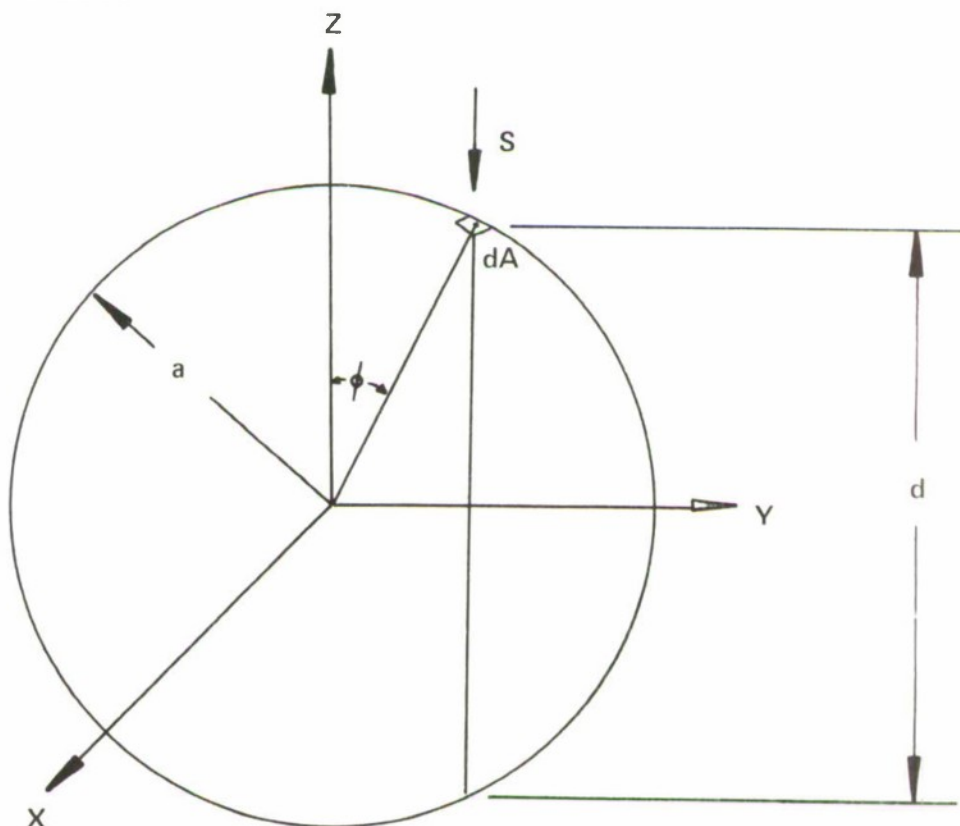


Figure 7. Coordinates of Interest for a Thermocouple Bead

The radiative flux incident on an element of surface area of the sphere  $dA = a^2 \sin \phi d\theta d\phi$  is dependent on the cosine of the angle between the incident flux and the normal to that element. The cosine of this angle is  $\cos \phi$ . The flux absorbed in passage through the sphere is  $S(1 - e^{-\alpha d})$ , where  $d = 2a \cos \phi$ . The total power  $P_a$  absorbed by the sphere is the sum over the surface area of the sphere of the product of the flux absorbed, the element of surface area, and  $-\cos \phi$ :

$$P_a = \int_{\phi=0}^{\pi/2} \int_{\theta=0}^{2\pi} S(1 - e^{-2\alpha a \cos \phi})(-\cos \phi)a^2 \sin \phi d\theta d\phi$$

This can be readily integrated to give

$$P_a = (2\alpha^2)^{-1} \pi S [1 - 2\alpha^2 a^2 - (1 + 2\alpha a)e^{-2\alpha a}]$$

The radiative flux emitted by the bead is given by the Stefan-Boltzmann relation  $S_e = (4\pi)^{-1} \sigma \epsilon T^4$ , where  $T$  is in degrees Kelvin, and  $\sigma$  is the Stefan-Boltzmann constant,  $5.67 \times 10^{-5}$  erg-cm<sup>-2</sup>-sec<sup>-1</sup>-(°K)<sup>-4</sup>. The emitted power  $P_e$  is the product of  $S_e$  and the surface area of the emitter:

$$P_e = \sigma \epsilon a^2 T^4$$

When the thermocouple bead is in thermal equilibrium, there is no accumulation of heat in the bead, and the power absorbed plus the power emitted equals zero. Equating  $P_a$  and  $P_e$  and solving for  $S$

$$S = \beta T^4 \quad (2)$$

where

$$\beta = 2\alpha^2 a^2 \sigma \epsilon (\pi)^{-1} [2\alpha^2 a^2 - 1 + (1 + 2\alpha a)e^{-2\alpha a}]^{-1} \quad (2)$$

To evaluate  $\beta$  for a specific thermocouple bead, the emissivity, the absorption coefficient, and the bead radius must be specified.

Consider the example of a Chromel-Alumel thermocouple such as that described in Section II. The radius of the bead is  $5 \times 10^{-2}$  cm. Chromel is 90% nickel, and Alumel is 94% nickel. Therefore, the values of  $\alpha$  and  $\epsilon$  are taken as those for oxidized nickel.<sup>9</sup> The emissivity is

<sup>9</sup>Handbook of Chemistry and Physics. 40 ed. Chemical Rubber Publishing Company, Cleveland, Ohio. 1959.

temperature dependent and may be represented by the following relation over  $400 \leq T \leq 1500^\circ \text{K}$ :

$$\epsilon = 0.27 + 5.00 \times 10^{-4}(T - 273)$$

where  $T$  is in degrees Kelvin ( $^\circ\text{C} + 273$ ). The absorption coefficient  $\alpha = 5 \times 10^4 \text{ cm}^{-1}$  represents an average over the wavelength span  $0.2\mu$  to  $4\mu$ , which covers the regions of maximum emission for most flames.<sup>10</sup> With these values

$$\beta = 4.87 \times 10^{-6} + 9.00 \times 10^{-9}(T - 273) \text{ erg-cm}^{-2}\text{-sec}^{-1}\text{-(}^\circ\text{K)}^{-4}$$

This can be rewritten as

$$\beta = 1.16 \times 10^{-13} + 2.15 \times 10^{-16}(T - 273) \text{ cal-cm}^{-2}\text{-sec}^{-1}\text{-(}^\circ\text{K)}^{-4}$$

since  $1.0 \text{ erg} = 2.3889 \times 10^{-8} \text{ cal}$ . Then equation (2) becomes

$$S = [1.16 \times 10^{-13} + 2.15 \times 10^{-16}(T - 273)] T^4 \text{ cal-cm}^{-2}\text{-sec}^{-1}$$

with  $T$  in degrees Kelvin.

The radiative flux of interest is that in excess of what is experienced under "ambient conditions." If the ambient temperature is taken as  $25^\circ\text{C} = 298^\circ\text{K}$ , the ambient flux is  $1.08 \times 10^{-3} \text{ cal-cm}^{-2}\text{-sec}^{-1}$ . Thus, a thermocouple recording a temperature  $T$  (in  $^\circ\text{K}$ , not that above the reference temperature) is exposed to a radiative flux of

$$\Delta S = \left\{ 1.16 \times 10^{-13} T^4 + 2.15 \times 10^{-16}(T - 273)T^4 - 1.08 \times 10^{-3} \right\} \text{ cal-cm}^{-2}\text{-sec}^{-1} \quad (3)$$

above ambient. A plot of  $\Delta S$  versus  $T$  is given in figure 8, with  $\Delta S$  given in  $\text{cal-cm}^{-2}\text{-sec}^{-1}$ , and  $T$  given in  $^\circ\text{C}$ .

It has been estimated that radiation is the primary source of heat flux within a flame,<sup>6,7,11</sup> and application of equation (3) is appropriate.

Thermocouple and heat flux measurements have been reported for flames from selected flame agents.<sup>11</sup> The thermocouple temperature versus time and heat

<sup>10</sup>Kelley, C. S. EATR 4555. Radiation Transfer Between Flame Burning Zone and Unburned Fuel. October 1971. UNCLASSIFIED Report.

<sup>11</sup>Smith, W. K. Burning Characteristics of Flame Weapon Fuels. US Naval Ordnance Test Station, China Lake. Technical Note 40604-3. April 1967. UNCLASSIFIED Report.

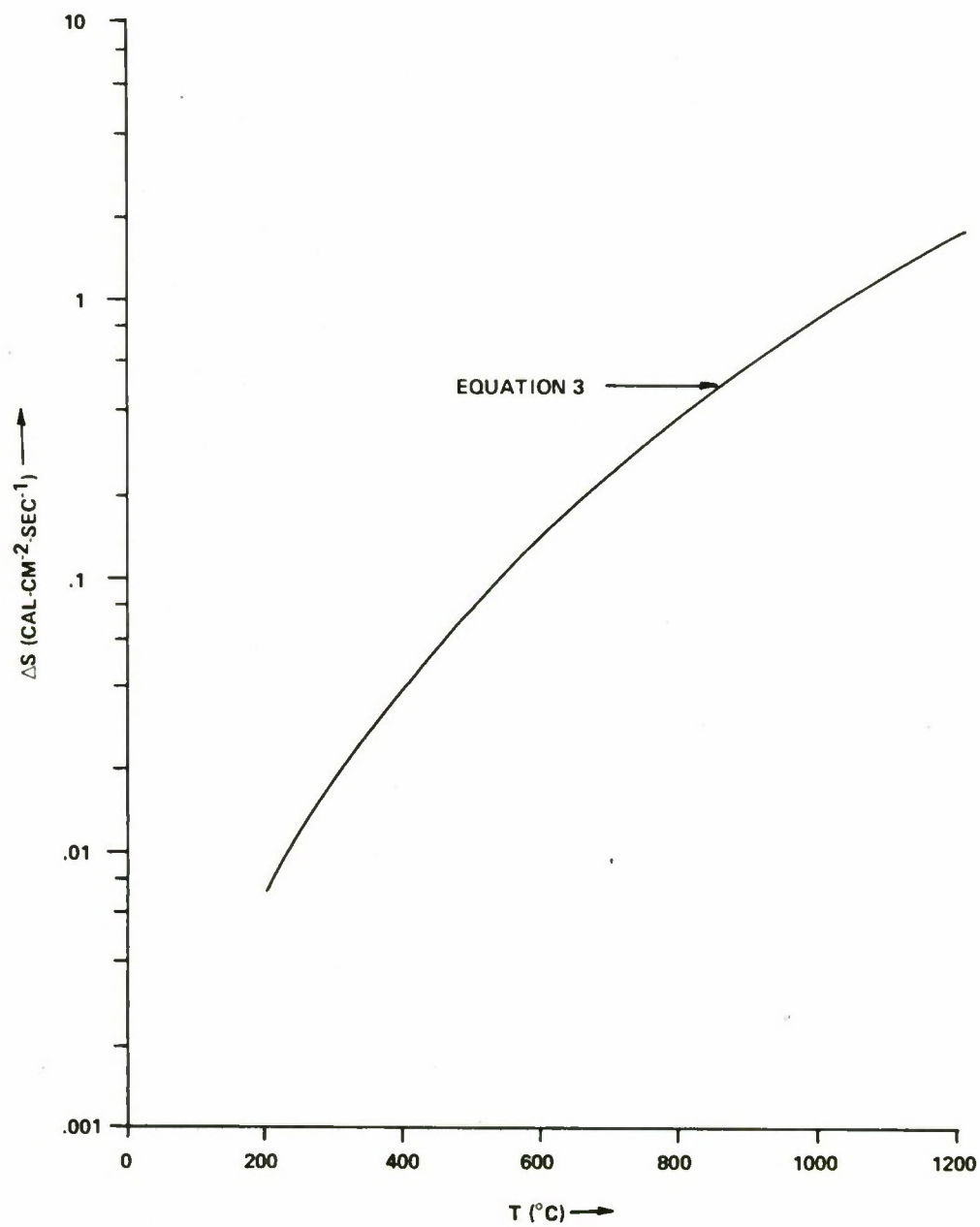


Figure 8. Theoretical Thermocouple Temperature Versus Incident Radiant Heat Flux

flux versus time data were taken at specific heights above various masses of the flame agent. These data provided a check on the accuracy of equation (3). Four temperatures were selected (as seen in the table). The times at which the thermocouple temperature versus time curves recorded these temperatures were noted. From these times, heat fluxes were determined from the corresponding heat flux versus time curves. The average heat flux for each of the four temperatures is given in the table, along with values of the heat flux calculated from equation (3). The indicated deviations in the experimental values indicate the average errors of the values from which the averages were calculated. As may be seen from the table, equation (3) is most accurate at higher temperatures, based upon these experimental data.

Table. Comparison of Equation (3) with Experimentally Determined Heat Flux Values

Temperature	Experimental heat flux	Calculated heat flux *
°C	cal-cm <sup>-2</sup> -sec <sup>-1</sup>	cal-cm <sup>-2</sup> -sec <sup>-1</sup>
538	0.5 ±0.1	0.1
704	0.6 ±0.02	0.3
816	0.8 ±0.06	0.5
926	0.9 ±0.1	0.8

\* Values of the heat flux calculated from equation (3).

In the derivation of equation (3), conduction of heat from the bead by the thermocouple wires was neglected. For most thermocouples, the dimensions of the bead and the wires are comparable, and conduction of heat by the wires may be appreciable. Also, in general, there will be a transfer of heat by conduction between the bead and the gases flowing past its surface. Because of the flickering nature of the flame, an assumption of thermal equilibrium may

not be representative. Thus, equation (3) represents a considerable simplification of the thermocouple response; in fact, the observation that the thermocouple temperature may be linearly scaled to the heat flux (Section III) indicates that the actual form of equation (3) is more complex.

## V. APPLICATIONS.

The criterion for ignition of a cellulosic target which is exposed to a time-dependent radiative flux  $S(t)$  is<sup>7</sup>

$$R = \int_0^{t_{ig}} [S(t)]^c dt \quad (4)$$

where the integral is evaluated from the moment the flux is applied,  $t = 0$ , to the time at which the target ignites,  $t = t_{ig}$ . The value of  $R$  depends on the physical properties of the target. It is constant, however, once the type, shape, and orientation of wood is specified.<sup>7</sup> The value of  $c$  for wood is 2.8.

The parallel between the thermocouple temperature and the heat flux it receives, as suggested by the experimental data in Section III and the theoretical treatment in Section IV, is taken advantage of here to predict the ignition time of a hypothetical wood target. The target is located 40 cm from the center of the base of the flame agent (25 grams 2% M4 thickened unleaded gasoline) and at an angle  $\phi$  from the vertical to the center of the base of the flame agent.

Because of the similar dependences of  $T_N$  and  $S_N$  on  $\phi$  [see Section III, figures 4 and 5, and equation (1)] the  $T(t) - 25$  curves were scaled to heat flux curves by the scale factor, equation (1). It is this scaled heat flux, raised to the 2.8 power, which is used in the integrand of equation (4).

We shall define a hypothetical ignition time,  $t'_{ig}$ , as follows. The  $S(t)$  curve at  $r = 40$  cm,  $\phi = 50^\circ$  is raised to the 2.8 power and integrated graphically throughout the entire duration of fuel burning. This integral is defined to be  $R$  for some hypothetical wood target. That is, the target, when placed at  $r = 40$  cm,  $\phi = 50^\circ$ , would ignite just as the fuel burns out. Next, the  $S(t)$  curves for all values of  $\phi$  were raised to the 2.8 power, and the integrals performed over time until the integrals equalled  $R$ . The resulting times are designated  $t'_{ig}$ .

The dependence of  $t'_{ig}$  on  $\phi$  is shown by the data points in figure 9. The solid line in figure 9 is a suggested curve through the data points. The value of  $t'_{ig}$  for  $\phi = 50^\circ$  is arbitrarily scaled to 1.0. It will be seen from figure 9 that the hypothetical ignition time is relatively constant for values of  $\phi$  up to about  $10^\circ$ . As  $\phi$  continues to increase beyond  $10^\circ$ , the hypothetical ignition time increases rapidly, until at  $\phi = 50^\circ$  it is about 15 times that at  $\phi = 0^\circ$ . This demonstrates the relatively large potential for target ignition at small values of  $\phi$  as compared to large values of  $\phi$ .

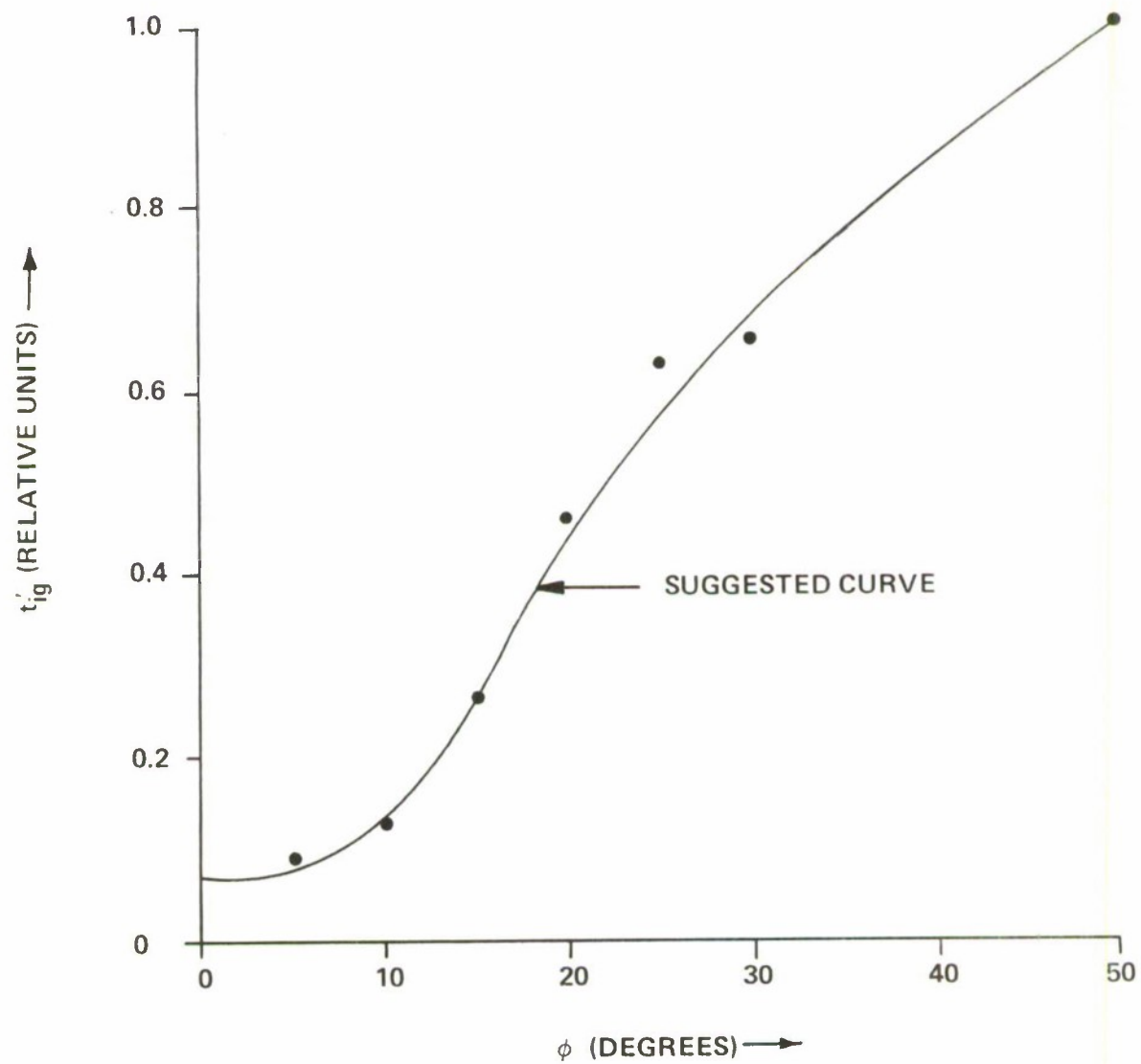


Figure 9. Dependence of Hypothetical Ignition Time on  $\phi$

Additionally, we performed thermocouple temperature versus time measurements at various heights,  $z$ , above 25 grams of the flame agent. Thermocouples were centered above the flame agent, which was allowed to burn to extinction. Ten measurements were taken at each height. The resulting temperature versus time data were broken into intervals of 20 seconds. The average thermocouple temperature during each 20-second interval for all 10 repetitions was computed and plotted. Slightly smoothed versions of these curves are presented in figure 10. The temperature decreases with increasing height. From the data in figure 10, the thermocouple temperature versus height at  $t = 2$ -, 4-, 5-, 6-, and 8-minutes were computed. These are presented in figure 11. From figure 11 it can be seen that the temperature versus height curves depend on whether  $z$  is greater than or less than about twice the pool diameter  $d$ . For  $z < 2d$  the temperature versus height decreases less rapidly than for  $z > 2d$ . Because these curves are time dependent, the dependences  $T(z)$ , which are of the form  $T = A(t) z^{B(t)}$ , will not be given in the form of equations. Any desired  $T(z, t)$  may be found either directly from the curves in figure 11 or by interpolation between these curves.

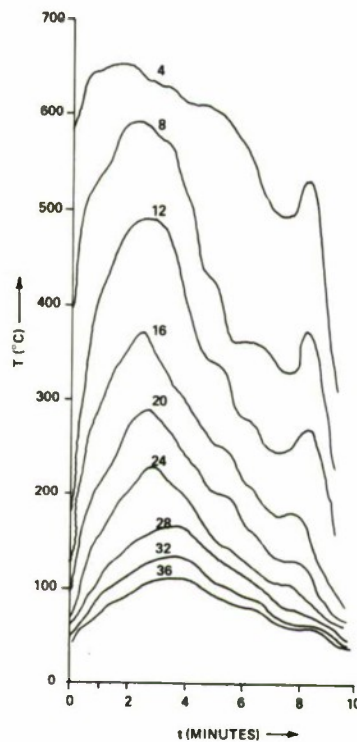


Figure 10. Dependence of Thermocouple Temperature  $T$  on Time  $t$  at Various Heights above the Flame Agent

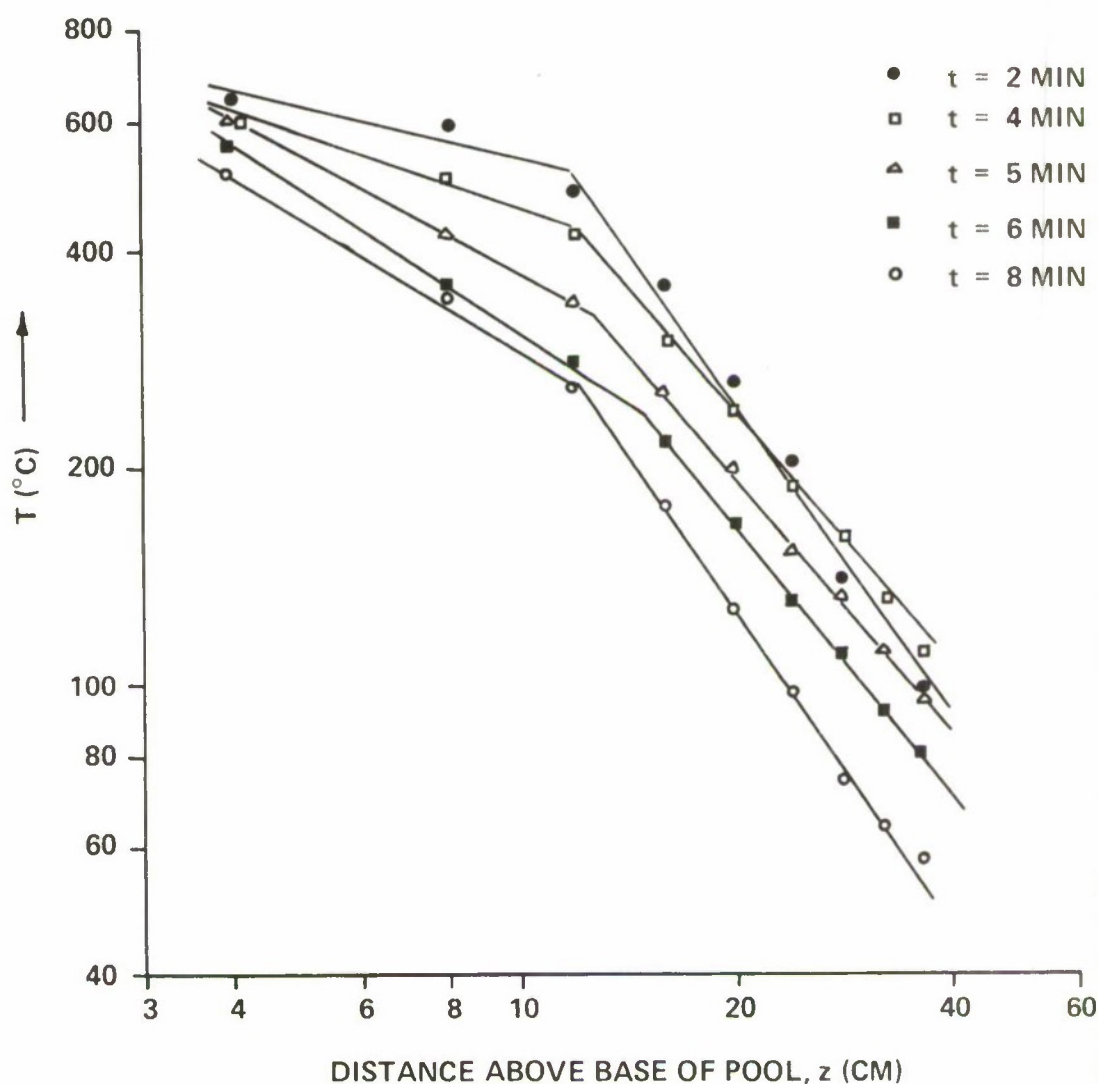


Figure 11. Dependence of Thermocouple Temperature  $T$  on Height  $z$  above the Flame Agent at Various Times During the Burning of the Agent

The thermocouple temperature rise above ambient ( $T - 25^\circ\text{C}$ ) is considered to parallel that of the heat flux, as indicated earlier in this report. Thus we may use the data of figure 10 to compute the dependence on  $z$  of a hypothetical ignition time  $t'_{ig}$ . The area under the  $[T(t) - 25^\circ\text{C}]^{2.8}$  curve for the  $z = 36$  cm case is taken as equal to  $R$  for some hypothetical wood. Then the ignition time for  $z = 36$  cm occurs as the flame agent is extinguished. Integrals of  $[T(t) - 25^\circ\text{C}]^{2.8}$  for the other heights were computed over  $0 \leq t \leq t'_{ig}$ . The resulting dependence of  $t'_{ig}$  on  $z$  is shown in figure 12.

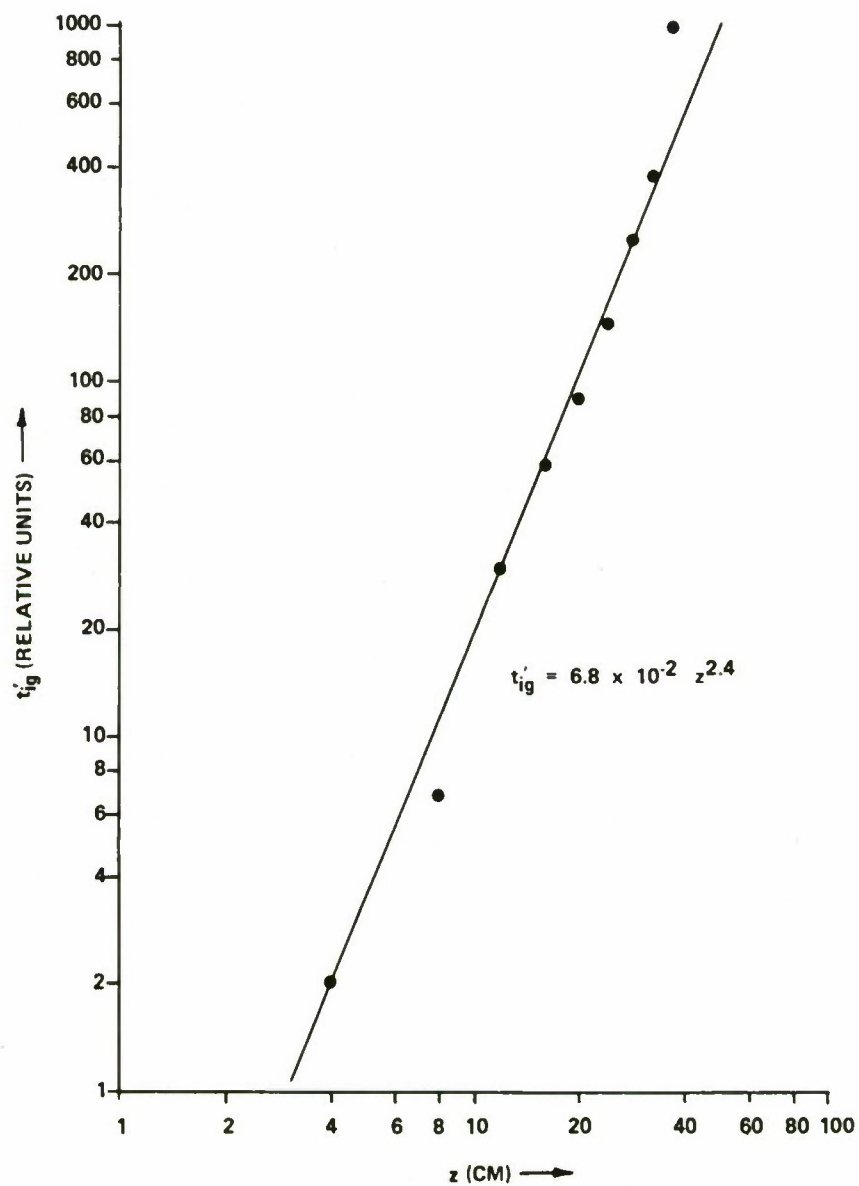


Figure 12. Dependence of Hypothetical Ignition Time  $t'_{ig}$  on Height  $z$  Above the Flame Agent

The dependence of  $t'_{ig}$  on  $z$  is well described by

$$t'_{ig} = 6.8 \times 10^{-2} z^{2.4}$$

over the range  $4 \text{ cm} \leq z \leq 36 \text{ cm}$ . Thus, the ignition time increases quite rapidly with height.

Either the above equation or figure 12 of this report, together with the data in figure 9 and figure 11 of Kelley's report,<sup>7</sup> provide all the information one needs for determining the spatial dependence of the hypothetical ignition time about a pool of burning Napalm. Figures 9 and 12 of this report give the hypothetical ignition time as a function of position about a 25-gram pool of burning Napalm, whereas figure 11 of Kelley's report<sup>7</sup> extends this dependence to any mass of Napalm ranging from 15 to 50 grams.

## VI. CONCLUSIONS.

Thermocouple temperature versus time measurements were performed on flames from burning pools of 25 grams of 2% M4 thickened unleaded gasoline. The thermocouples were located 40 cm from the center of the base of the pool and at various angles  $\phi$  from the flame symmetry axis.

From these measurements, the dependence of the thermocouple temperature on  $\phi$  was determined. The dependence is quite similar to that of the radiative plus convective heat flux for other similar flame agents: a rapid decrease up to  $\phi \simeq 30^\circ$  and then a far less rapid decrease.

Using the similarity of the dependence on  $\phi$  of the thermocouple temperature and heat flux, the thermocouple temperature is converted to heat flux by an empirical scale factor. The dependence of the thermocouple temperature on radiative flux is derived for the ease of small conductive and convective heat losses.

From the thermocouple temperature data, the dependence on  $\phi$  of the time to ignition for a hypothetical wood target is predicted. With increasing  $\phi$ , the ignition time is relatively constant up to  $\phi \simeq 10^\circ$ , and it then increases rapidly. This ignition time depends on the height above the flame agent, and is found to obey a power law, with the ignition time increasing with increasing height.

Ignition experiments were performed on balsa, pine, maple, and oak. Both the time-dependent heat flux intensity and the time to ignition were measured. They are predicted to be related by an equation involving the density and spectral absorbance of the wood. This equation is confirmed experimentally and provides a criterion for the effectiveness of a specific heat flux in the ignition of wood.

BLANK

### LITERATURE CITED

1. Wilkes, G. B. NDRC Contract. Final Report. Symbol No. 574. Radiation Characteristics of Burning Incendiary Materials. June 1942. UNCLASSIFIED Report.
2. Koch, H. W. Vergleichmessungen von Temperaturen and Wärmestromdichten an Brandstoffen. Technische Mitteilung ISL-T 40/67, Deutsch - Französisches Forschungsinstitut Saint-Louis 10, 11 (1967).
3. Kelley, C. S. EATR 4436. The Use of Spatially-Separated Series-Linked Thermocouples in Flame Evaluation. August 1970. UNCLASSIFIED Report.
4. Brown, R. E., Garfinkle, D. R., and Andersen, W. H. Shock Hydrodynamics, Inc. Final Report SHI-6245-3. Contract DAAA-15-69-C-0301. Evaluation Techniques for Flame and Incendiary Agents. June 1970. UNCLASSIFIED Report.
5. Kelley, C. S. EATR 4492. Dependence of Heat Flux (Radiative Plus Convective) From Burning Flame Agents on the Angle from the Flame Symmetry Axis. February 1971. UNCLASSIFIED Report.
6. Welker, J. R., and Sliepcevich, C. M. Final Report. Contract DAAA-15-67-C-0074. Susceptibility of Potential Target Components to Defeat by Thermal Action (U). July 1970. UNCLASSIFIED Report.
7. Kelley, C. S. EATR 4539. Piloted Ignition Times for Cellulosic Solids Exposed to Time-Dependent Heat Fluxes. August 1971. UNCLASSIFIED Report.
8. Technical Documentary Report No. ATL-TDR-64-34. Instantaneous Preparation of Flame Fuels for Fire Bombs, Prepared Under Contract No. AF 08(635)-3638, AFSC Project 670A, by Westco Research, a Division of The Western Company of North America. January 1964. CONFIDENTIAL Report.
9. Handbook of Chemistry and Physics. 40 ed. Chemical Rubber Publishing Company, Cleveland, Ohio. 1959.
10. Kelley, C. S. EATR 4555. Radiation Transfer Between Flame Burning Zone and Unburned Fuel. October 1971. UNCLASSIFIED Report.
11. Smith, W. K. Burning Characteristics of Flame Weapon Fuels. US Naval Ordnance Test Station, China Lake, Technical Note 40604-3. April 1967. UNCLASSIFIED Report.

12. Smith, W. K. Ignition of Edges and Corners of Wood. Naval Weapons Center, China Lake. Technical Note 40604-18. June 1971. UNCLASSIFIED Report.

13. Wesson, H. R., Welker, J. R., and Sliepceovich, C. M. The Piloted Ignition of Wood by Thermal Radiation. Combustion and Flame 16, 303-310 (1971).

## APPENDIX

### PRESENTATION OF RESULTS OF EXPERIMENTS DESIGNED TO INVESTIGATE THE VALIDITY OF EQUATION (5)

The criterion for ignition of a cellulosic solid that is exposed to time-dependent radiation is given by equation (4) of the text and it may be rewritten as

$$\int_0^{t_{ig}} [S(t)]^{2.8} dt = 35\rho^{0.9}\alpha^{-2.8} \quad (5)$$

The density  $\rho$  and the optical absorbance  $\alpha$  are the physical properties of the solid that determine the ignition time.<sup>7</sup>

Samples of balsa, pine, maple, and oak were cut to blocks of dimensions 1/2 by 1/2 by 3/8 inches. A small hole was drilled through the center of the largest face of each of the samples, and the edges and corners were masked with aluminum foil to keep them from igniting prior to the faces,<sup>12</sup> as they have been observed to do. Samples were oven-dried at 110°C for 17 hours prior to testing. The sources of heat flux for the tests were the same as those described in Section II of the text. The heat flux sensors were Chromel-Alumel thermocouples whose wires were insulated with asbestos and then fitted inside pyrex tubes. The thermocouple beads and about 1/4 inch of the lead wires were exposed at the ends of the tubes. The exposed beads of the thermocouple junctions which were passed through the closely fitting holes in the wood samples protruded about 1/16 inch from the centers of the sample faces that were exposed to the heat flux. The thermocouple wires thereby served to support the samples.

The thermocouples were positioned above the flame agent so as to be in direct contact with the flame. The temperature rise above ambient ( $T - 25^\circ\text{C}$ ) was recorded for each thermocouple, and the time of ignition was noted on the Visicorder recording strip.

In the first set of experiments, 13 balsa samples were ignited. In the second set of experiments, two balsa samples, two pine samples, three maple samples, and two oak samples were ignited. The first set of experiments provided a measure of the constancy of

$$\int_0^{t_{ig}} [S(t)]^{2.8} dt$$

---

<sup>12</sup>Smith, W. K. Ignition of Edges and Corners of Wood. Naval Weapons Center, China Lake. Technical Note 40604-18. June 1971. UNCLASSIFIED Report.

for a single wood type. The second set of experiments provided a check on the constancy of

$$\rho^{-0.9} \alpha^{2.8} \int_0^{t_{ig}} [S(t)]^{2.8} dt$$

for four wood types.

The heat flux  $S$  may be written as  $S = C_1 (T - 25)$ , where  $C_1$  is the scale factor for conversion of thermocouple temperature to heat flux (discussed in text). The deflection  $h$  of the Visicorder trace is linearly related to  $(T - 25)$ . Thus  $(T - 25) = C_2 h$ , so that  $S(t) = C_1 C_2 h(t)$ , and

$$\int_0^{t_{ig}} [S(t)]^{2.8} dt = C_1^{2.8} \int_0^{t_{ig}} [T(t) - 25]^{2.8} dt = [C_1 C_2]^{2.8} \int_0^{t_{ig}} [h(t)]^{2.8} dt \quad (6)$$

Figures A-1, A-2, and A-3 give  $[h(t)]^{2.8}$  for balsa. The samples' positions were changed from test to test in order to vary the heat flux incident upon them. Because the Visicorder scale factor  $C_2$  varied from channel to channel, the graphs were grouped by the channel on which they were recorded. To obtain  $[T(t) - 25]^{2.8}$ , each trace in the figures must be multiplied by the factors listed on the figures. The ignition time is indicated by the termination of the graphs.

The integrals over time of  $[T(t) - 25]^{2.8}$  are presented in table A-I. The first column locates the particular test and channel, the second column lists  $\int_0^{t_{ig}} [h(t)]^{2.8} dt$ , and the third column lists  $C_2^{2.8}$ . The fourth column gives

$$\int_0^{t_{ig}} [T(t) - 25]^{2.8} dt \quad (7)$$

which may be rewritten by equation (6) as

$$C_1^{2.8} \int_0^{t_{ig}} [S(t)]^{2.8} dt = 35 C_1^{2.8} \rho^{0.9} \alpha^{2.8}$$

In this set of experiments,  $C_1$ ,  $\rho$ , and  $\alpha$  were constant so that equation (7) is expected to be constant. From the values in table A-I

$$\int_0^{t_{ig}} [T(t) - 25]^{2.8} dt = 5.8$$

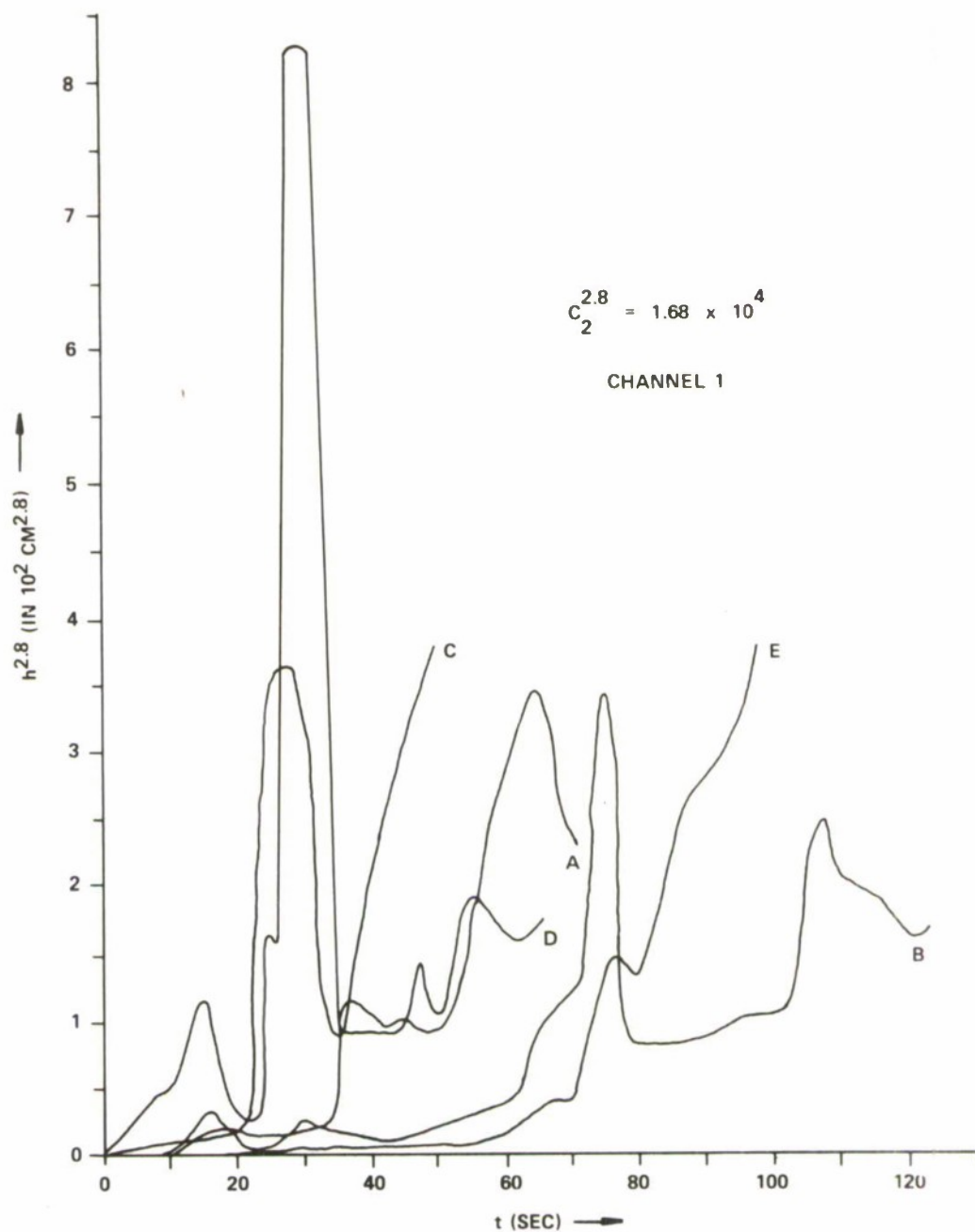


Figure A-1. Time Dependence of  $h^{2.8}$ , Measured on Visicorder Channel 1, for Balsa

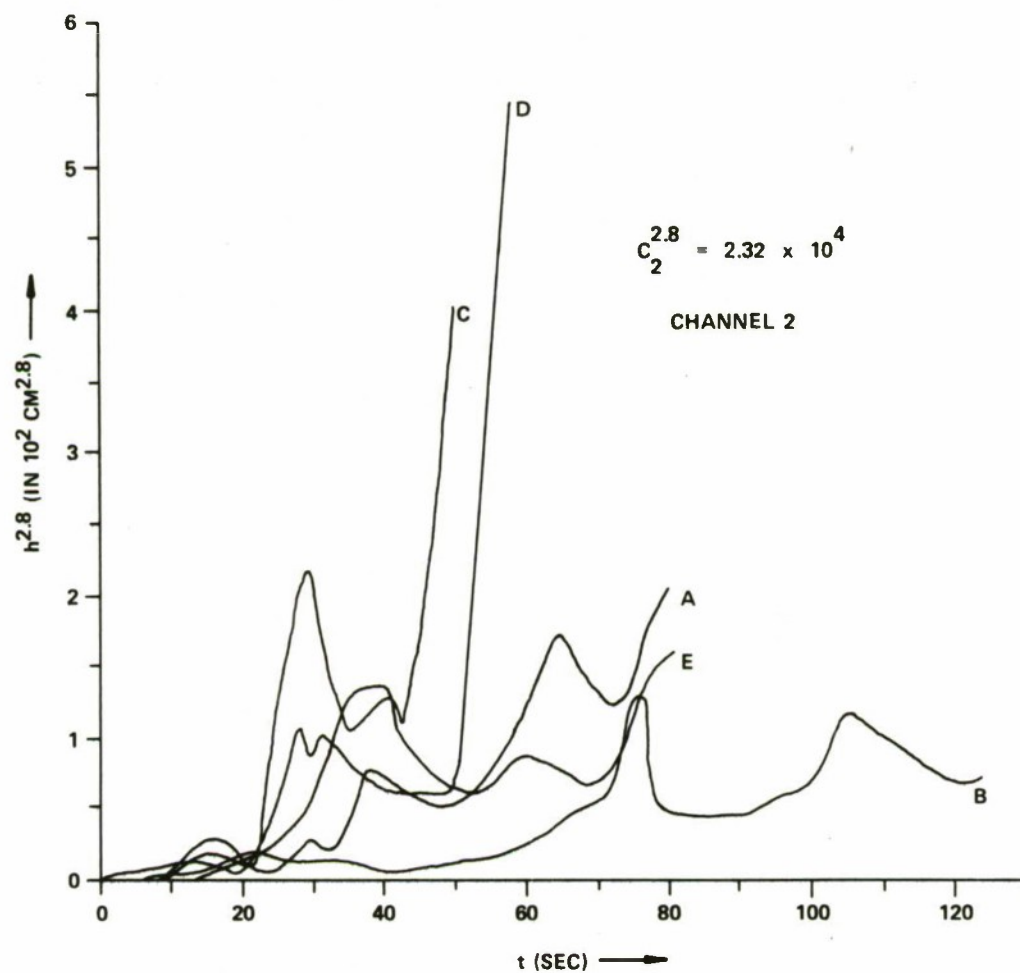


Figure A-2 Time Dependence of  $h^{2.8}$  Measured on Visicorder Channel 2, for Balsa

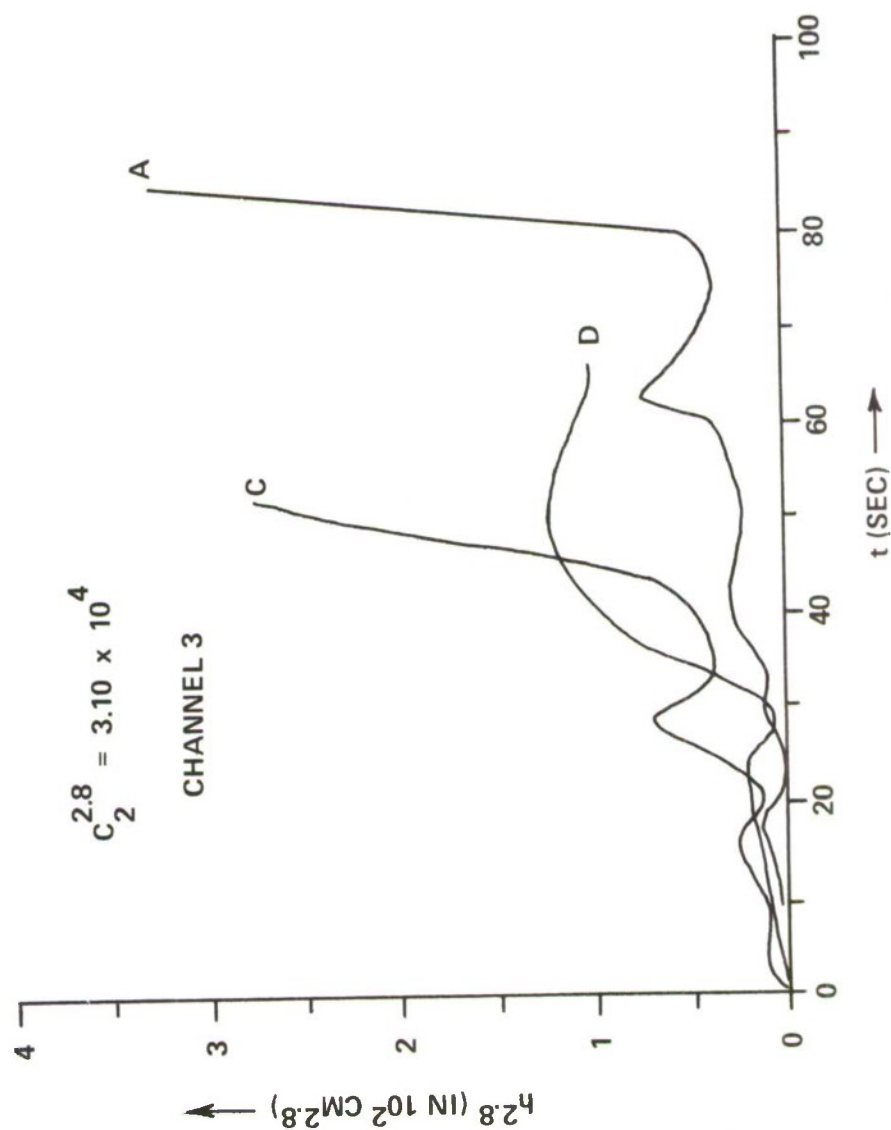


Figure A-3. Time Dependence of  $h^{2.8}$  Measured on Visicorder  
Channel 3, for Balsa

Table A-1. Results of Experiments on the Piloted Ignition of Balsa

Channel; test		$\int_0^{t_{ig}} [h(t)]^{2.8} dt^*$	$C_2^{2.8**}$	$\int_0^{t_{ig}} [T(t)-25]^{2.8} dt^\dagger$
1	A	322	1.68	5.41
1	B	358		6.02
1	C	333		5.60
1	D	446		7.48
1	E	323		5.43
2	A	234	2.32	5.43
2	B	236		5.48
2	C	246		5.71
2	D	219		5.08
2	E	244		5.66
2	H	287	3.10	6.66
3	A	132		4.10
3	C	140		4.34
3	D	175		5.43
3	H	291		9.02

\* Units of  $\text{cm}^{2.8}\text{-sec}$ \*\* Units of  $10^4 (\text{°C}\text{-cm}^{-1})^{2.8}$ † Units of  $10^6 (\text{°C})^{2.8}\text{-sec}$

with an average deviation of 0.8. Thus equation (5) is found to be accurate to within 14% for these tests.

The results of the second set of experiments are given in figures A-4, A-5, and A-6. Again, the quantity  $[h(t)]^{2.8}$  is plotted in each figure, and the tests are grouped by Visicorder channel in the figures. In these series of tests, the quantity

$$\rho^{-0.9} \alpha^{2.8} \int_0^{t_{ig}} [T(t) - 25]^{2.8} dt = 35C_1^{-2.8} \quad (8)$$

is predicted to be constant, regardless of wood type.

The quantities  $\rho$ ,  $\alpha$ ,  $\rho^{-0.9}$ , and  $\alpha^{2.8}$  are listed in table A-II for the various wood types. Both  $\rho$  and  $\alpha$  for these and other wood types may be found elsewhere.<sup>6</sup>

The last column of table A-III presents the values of the left side of equation (8) for the samples tested. From these values

$$\rho^{-0.9} \alpha^{2.8} \int_0^{t_{ig}} [T(t) - 25]^{2.8} dt = 12.0$$

with an average deviation of 4.6. Thus, for this set of experiments, equation (5) is found to be accurate to within 38%. Combining this accuracy and that of the first set, and assigning a weight factor for each set equal to the number of tests in each set, the overall accuracy of equation (5) is to within 23%.

These experiments confirm the empirical criterion, equation (5) for the ignition of wood exposed to a time dependent heat flux. This ignition criterion was predicted<sup>7</sup> from the experimental results of the piloted ignition of wood exposed to a constant heat flux.<sup>13</sup>

<sup>13</sup> Wesson, H. R., Welker, J. R., and Sliepcevich, C. M. The Piloted Ignition of Wood by Thermal Radiation. Combustion and Flame 16, 303-310 (1971).

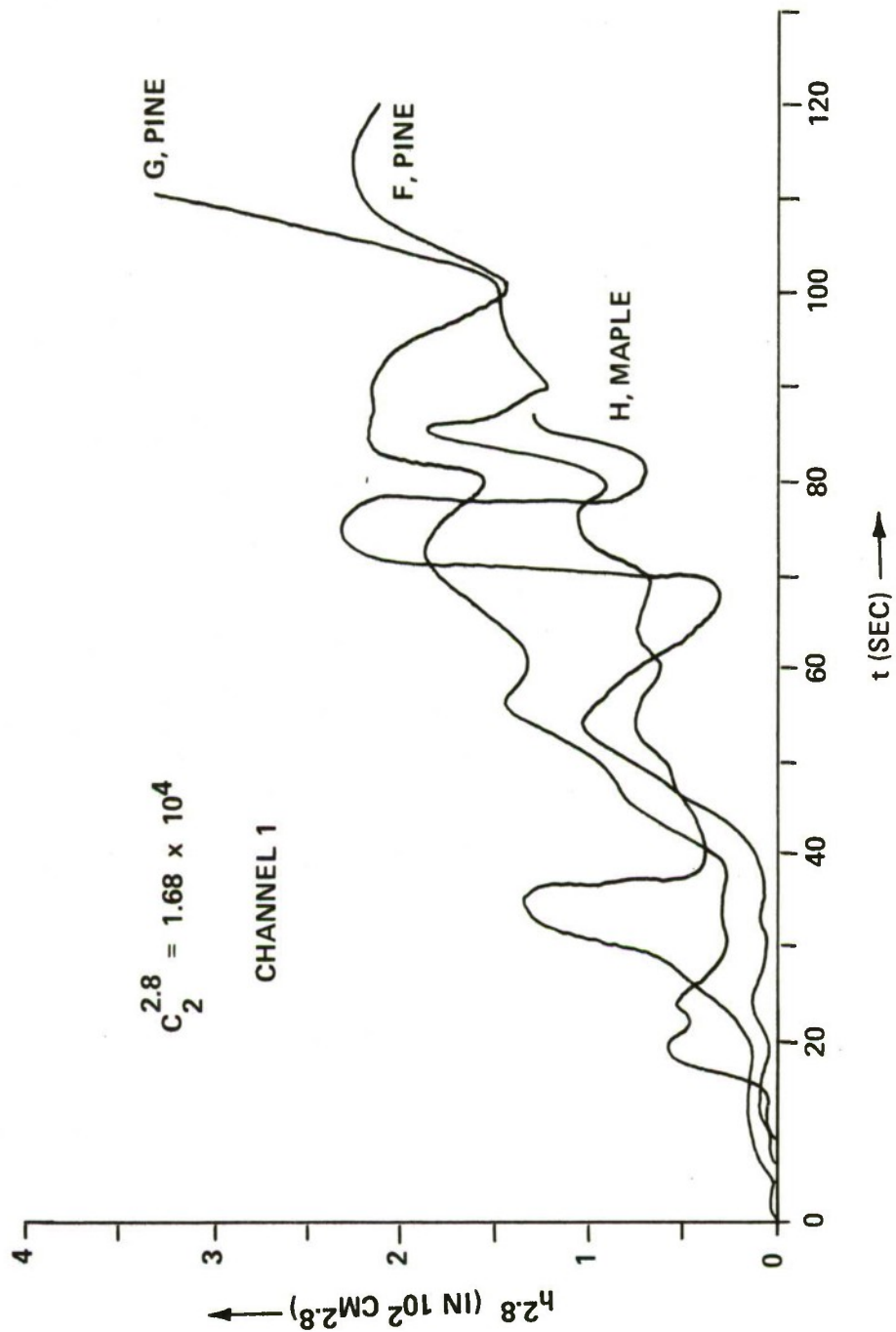


Figure A-4. Time Dependence of  $h_{2.8}$ , Measured on Visicorder Channel 1, for Pine and Maple

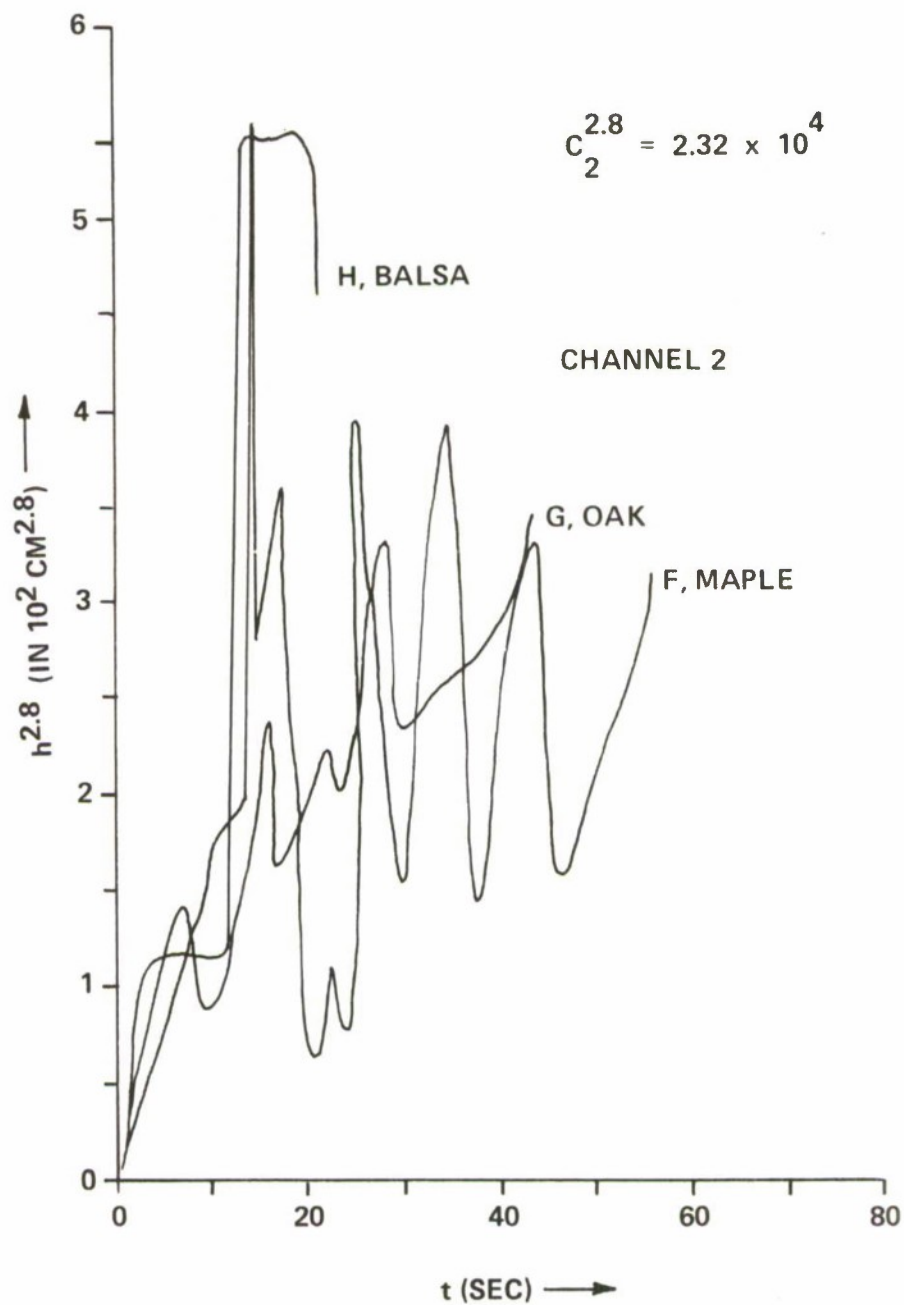


Figure A-5. Time Dependence of  $h^{2.8}$ , Measured on Visicorder Channel 2, for Balsa, Maple, and Oak

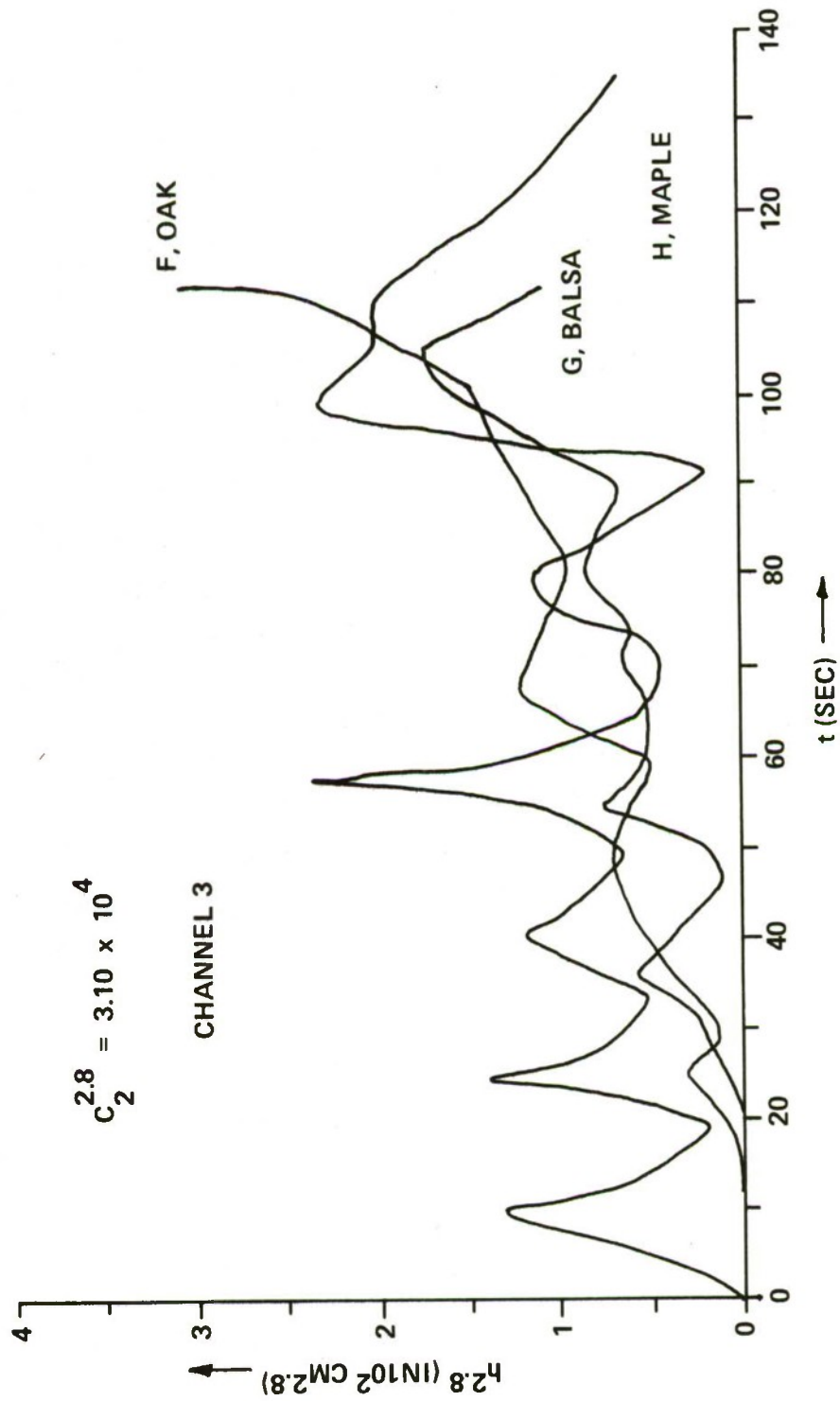


Figure A-6. Time Dependence of  $h^{2.8}$ , Measured on Visicorder  
Channel 3, for Balsa, Maple, and Oak

Table A-II. Physical Parameters Which Influence the Ignition Time for Specific Wood Types

Wood	Density *	Absorbance **	$\rho^{-0.9\dagger}$	$\alpha^{2.8**}$
Balsa	0.09	0.75	8.77	0.421
Pine	0.34	0.76	2.64	0.439
Maple	0.67	0.76	1.43	0.439
Oak	0.70	0.77	1.38	0.457

\* Units of  $\text{gm-cm}^{-3}$

\*\* Unitless

† Units of  $(\text{gm-cm}^{-3})^{2.8}$

Table A-III. Results of Experiments on the Piloted Ignition of  
Balsa, Pine, Maple and Oak

Wood	Channel; test		$\int_0^{t_{ig}} [h(t)]^{2.8} dt^*$	$C_2^{2.8**}$	$\int_0^{t_{ig}} [T(t)-25]^{2.8} dt^\dagger$	Average <sup>§</sup> $\rho^{-0.9} \alpha^{2.8} \int_0^{t_{ig}} [T(t)-25]^{2.8} dt$
Pine	1	F	698	1.68	11.8	} 11.4
Pine	1	G	468	1.68	7.87	
Maple	1	H	229	1.68	3.86	} 7.75
Maple	2	F	559	2.32	13.0	
Maple	3	H	663	3.10	19.7	
Oak	2	G	459	2.32	10.7	} 7.73
Oak	3	F	441	3.10	13.7	
Balsa	Data taken from table A-I				5.8	21.3

\* Units of  $\text{cm}^{2.8}\text{-sec}$

\*\* Units of  $10^4 (\text{°C}\text{-cm}^{-1})^{2.8}$

† Units of  $10^6 (\text{°C})^{2.8}\text{-sec}$

§ Units of  $10^6 (\text{gm}\text{-cm}^{-3})^{-0.9} (\text{°C})^{2.8}\text{-sec}$

## DISTRIBUTION LIST 3

Agency	Copies	Agency	Copies
EDGEMOOD ARSENAL		MANUFACTURING TECHNOLOGY DIRECTORATE	
OFFICE OF THE COMMANDER		Chemical & Plants Division	
Associate Tech Director for Engineering		ATTN: SMUEA-MTC	1
ATTN: SMUEA-TD-E	1	DEPARTMENT OF DEFENSE	
FOREIGN INTELLIGENCE OFFICE		Defense Documentation Center	12
ATTN: SMUEA-FI	3	Cameron Station	
LEGAL OFFICE, ATTN: SMUEA-LE	1	Alexandria, VA 22314	
SAFETY OFFICE, ATTN: SMUEA-SA	1	Defense Intelligence Agency	
Director, USAMUCOM Operations Research Group		ATTN: DIAAP-7E	1
ATTN: AMSMU-DR	1	Washington, DC 20301	
Record Set, RIIA, APG-EA, Bldg. 5179	1		
Authors Copy, Chemical Laboratory	2	DEPARTMENT OF THE ARMY	
TECHNICAL SUPPORT DIRECTORATE		HQ DAHD	
Technical Releases Division		ATTN: DAHD-CNS	1
ATTN: SMUEA-TS-R	2	Washington, DC 20310	
Technical Library Division		OFFICE OF THE SURGEON GENERAL	
ATTN: SMUEA-TS-L	10	HQ DA (SGRD-MDP-B)	1
Test & Evaluation Division		Washington, DC 20314	
ATTN: SMUEA-TS-T	1	US ARMY MATERIEL COMMAND	
PRODUCT ASSURANCE DIRECTORATE		Commanding General	
Product Assurance Test Division		US Army Materiel Command	
ATTN: SMUEA-PA-T	1	ATTN: AMCSF	1
Product Quality Assurance Division		ATTN: AMCRD-WB	1
ATTN: SMUEA-PA-QW	1	Washington, DC 20315	
CHEMICAL LABORATORY		Commanding General	
Chemical Research Division		Deseret Test Center	
ATTN: SMUEA-CL-C	1	ATTN: Technical Library	3
ATTN: SMUEA-CL-CA	1	Bldg 100, Soldier's Circle	
ATTN: SMUEA-CL-CO	1	Fort Douglas, UT 84113	
ATTN: SMUEA-CL-CP	1	US ARMY MUNITIONS COMMAND	
Physical Research Division		Commanding General	
ATTN: SMUEA-CL-P	1	US Army Munitions Command	
ATTN: SMUEA-CL-PA	1	ATTN: AMSMU-MS-CH	1
ATTN: SMUEA-CL-PR	2	ATTN: AMSMU-QA-MR	1
BIOMEDICAL LABORATORY		ATTN: AMSMU-RE-CN	1
ATTN: SMUEA-BL	1	ATTN: AMSMU-RE-RT	1
ATTN: SMUEA-BL-M	7	ATTN: AMSMU-XM	1
Human Factors Group		Dover, NJ 07801	
ATTN: SMUEA-BL-H	1		
Biophysics Division			
ATTN: SMUEA-BL-B	1		
ATTN: SMUEA-BL-BB	1		
ATTN: SMUEA-BL-BW	1		
Medical Research Division			
ATTN: SMUEA-BL-RC	1		
DEV & ENG DIRECTORATE			
ATTN: SMUEA-DE	1		
Engineering Analysis Office			
ATTN: SMUEA-DE-N	1		
System Engineering/Configuration Management Office			
ATTN: SMUEA-DE-SM	1		
Maintenance Engineering Division			
ATTN: SMUEA-DE-EF	1		
Defense Systems Division			
ATTN: SMUEA-DE-DP	1		

## DISTRIBUTION LIST 3 (Con'd)

Agency	Copies
<b>CONARC</b>	
United States Army Infantry School Bde & Bn Dept, Cbt Spt Gp ATTN: Chmn, NBC Committee Fort Benning, GA 31905	1
Commandant USA Chemical Center & School ATTN: ATSCM-A-D Fort McClellan, AL 36201	1
<b>DEPARTMENT OF THE NAVY</b>	
Commanding Officer Naval Explosive Ordnance Disposal Facility ATTN: Code ES21 Indian Head, MD 20640	1
Naval Post Graduate School Monterey, CA 93940	1
Commander Naval Weapons Center ATTN: Code 753 (Tech Lib) ATTN: Code 4060 (W.K. SMith) China Lake, CA 93555	1 1
<b>US MARINE CORPS</b>	
Commandant, USMC Hq. US Marine Corps ATTN: Code A04F Washington, DC 20380	2

## DISTRIBUTION LIST FOR DD 1473's

Agency	Copies
Technical Support Directorate ATTN: SMUIA-TS-R ATTN: SMUIA-TS-L	1 2
Management Information Systems Directorate ATTN: SMUIA-MI	1

UNCLASSIFIED

Security Classification

## DOCUMENT CONTROL DATA - R &amp; D

(Security classification of title, body of abstract and indexing annotation must be entered when the overall report is classified)

1. ORIGINATING ACTIVITY (Corporate author) Cdr. Edgewood Arsenal ATTN: SMUEA-CL-PRF Aberdeen Proving Ground, Maryland 21010		2a. REPORT SECURITY CLASSIFICATION UNCLASSIFIED	
		2b. GROUP NA	
3. REPORT TITLE  THERMOCOUPLE MEASUREMENT OF HEAT FLUX AND APPLICATION TO IGNITION OF WOOD			
4. DESCRIPTIVE NOTES (Type of report and inclusive dates) This work was started in June 1971 and completed in August 1971.			
5. AUTHOR(S) (First name, middle initial, last name)  C. Stuart Kelley, Ph. D., and Aldean Bengé			
6. REPORT DATE March 1973		7a. TOTAL NO. OF PAGES 43	7b. NO. OF REFS 13
8a. CONTRACT OR GRANT NO.  b. PROJECT NO. 1W562603A065  c.  d.		9a. ORIGINATOR'S REPORT NUMBER(S)  EATR 4696  9b. OTHER REPORT NO(S) (Any other numbers that may be assigned this report)	
10. DISTRIBUTION STATEMENT  Approved for public release; distribution unlimited.			
11. SUPPLEMENTARY NOTES Flame, incendiary, and smoke technology		12. SPONSORING MILITARY ACTIVITY	
13. ABSTRACT  Measurements reported here on flames from thickened hydrocarbons indicate that close to, but outside, the flame outline the thermocouple temperature can be converted to the heat flux emitted by the flame. From the thermocouple data, the dependence of the time to ignition for a wood target outside the flame on the angle from the flame symmetry axis is established. For angles less than about 10 degrees, the ignition time is relatively constant; for larger angles, it increases rapidly. The dependence of the time to ignition on the height above the flame agent is also established; it increases rapidly with increasing height. Measurements reported here on the ignition of wood confirm the predicted dependence of the ignition time on the time-dependent incident heat flux intensity.			
14. KEYWORDS  Flames Heat flux measurement Hydrocarbon flame Thermocouples Ignition of wood			

DD FORM 1473  
1 NOV 55REPLACES DD FORM 1473, 1 JAN 54, WHICH IS  
OBSOLETE FOR ARMY USE.

43

UNCLASSIFIED

Security Classification

14.

### KEY WORDS

**LINK A**

LINK 8

LINK C

	NAME	DATE	ROLE
1	JOHN D. BROWN	10/10/68	CHIEF OF POLICE
2	JAMES E. HARRIS	10/10/68	SERIALS UNIT
3	WILLIAM J. MURPHY	10/10/68	INVESTIGATIVE DIVISION
4	ROBERT L. TAYLOR	10/10/68	LABORATORY
5	MICHAEL A. WILSON	10/10/68	TRAINING DIVISION
6	CHARLES F. YOUNG	10/10/68	COMMUNITY RELATIONS
7	EDWARD G. ZIMMERMAN	10/10/68	RECORDS & COMMUNICATIONS
8	HENRY J. ALLEN	10/10/68	ADMINISTRATIVE SERVICES
9	BETTY S. COOPER	10/10/68	CLERICAL SUPPORT
10	FRANK R. EVANS	10/10/68	PROPERTY CLERK
11	LUCAS M. GREEN	10/10/68	OFFICE ASSISTANT
12	DAVID K. HAMILTON	10/10/68	RECEPTIONIST
13	ANNE C. JACKSON	10/10/68	FILE CLERK
14	GEORGE P. KING	10/10/68	TRAINING OFFICER
15	HELEN I. LEVY	10/10/68	LABORATORY ASST.
16	IRVING N. MILLER	10/10/68	INVESTIGATIVE DIVISION
17	JOSEPH O. NELSON	10/10/68	CHIEF OF POLICE
18	KAROL ANN OLIVER	10/10/68	CLERICAL SUPPORT
19	LEONARD Q. PERKINS	10/10/68	LABORATORY
20	MARGARET R. QUINN	10/10/68	RECORDS & COMMUNICATIONS
21	NATHAN S. ROSS	10/10/68	ADMINISTRATIVE SERVICES
22	OPHELIA T. SHAW	10/10/68	CLERICAL SUPPORT
23	PETER V. STEVENSON	10/10/68	TRAINING DIVISION
24	RUTH W. THOMPSON	10/10/68	PROPERTY CLERK
25	SCOTT X. UNDERWOOD	10/10/68	OFFICE ASSISTANT
26	TERRA Y. VAUGHN	10/10/68	RECEPTIONIST
27	UPTON Z. WEBSTER	10/10/68	FILE CLERK
28	VICTORIA A. WHITE	10/10/68	TRAINING OFFICER
29	WALTER B. BLACK	10/10/68	LABORATORY ASST.
30	XAVIER C. BLUE	10/10/68	INVESTIGATIVE DIVISION
31	YVETTE D. GOLD	10/10/68	CHIEF OF POLICE
32	ZACHARY E. IRVING	10/10/68	CLERICAL SUPPORT
33	AARON F. KELLEY	10/10/68	LABORATORY
34	BABYLOON G. LONG	10/10/68	RECORDS & COMMUNICATIONS
35	CASSIUS H. MITCHELL	10/10/68	ADMINISTRATIVE SERVICES
36	DANIEL J. NICHOLS	10/10/68	CLERICAL SUPPORT
37	EUGENE K. ORTEGA	10/10/68	TRAINING DIVISION
38	FREDERICK L. PARKER	10/10/68	PROPERTY CLERK
39	GEOFFREY M. REYNOLDS	10/10/68	OFFICE ASSISTANT
40	HARRISON N. SIMMONS	10/10/68	RECEPTIONIST
41	IDA B. TATE	10/10/68	FILE CLERK
42	JACOB C. TURNER	10/10/68	TRAINING OFFICER
43	KENNETH D. URBAN	10/10/68	LABORATORY ASST.
44	LUCILLE E. VAN DYKE	10/10/68	INVESTIGATIVE DIVISION
45	MARTIN F. WALLACE	10/10/68	CHIEF OF POLICE
46	NANCY G. WARREN	10/10/68	CLERICAL SUPPORT
47	OSCAR H. WATKINS	10/10/68	LABORATORY
48	PATRICK I. WEST	10/10/68	RECORDS & COMMUNICATIONS
49	QUENTIN J. WOOD	10/10/68	ADMINISTRATIVE SERVICES
50	ROSAMUND K. YORK	10/10/68	CLERICAL SUPPORT
51	STEPHEN L. ZUCKERMAN	10/10/68	TRAINING DIVISION
52	THERESA M. ADAMS	10/10/68	PROPERTY CLERK
53	UDYNN N. BAKER	10/10/68	OFFICE ASSISTANT
54	VANCE O. CAMPBELL	10/10/68	RECEPTIONIST
55	VERNON P. CARTER	10/10/68	FILE CLERK
56	WILLIAM Q. CHASE	10/10/68	TRAINING OFFICER
57	XENIA R. CLARK	10/10/68	LABORATORY ASST.
58	YVES S. COLE	10/10/68	INVESTIGATIVE DIVISION
59	ZACHARIAH T. DAVIDSON	10/10/68	CHIEF OF POLICE
60	ADRIAN U. EDWARDS	10/10/68	CLERICAL SUPPORT
61	BENJAMIN V. FARROW	10/10/68	LABORATORY
62	CARROLL W. GIBBS	10/10/68	RECORDS & COMMUNICATIONS
63	DANIEL X. GRANT	10/10/68	ADMINISTRATIVE SERVICES
64	ELEANOR Y. HARVEY	10/10/68	CLERICAL SUPPORT
65	FREDERICK Z. HENDERSON	10/10/68	TRAINING DIVISION
66	GEOFFREY A. HOWARD	10/10/68	PROPERTY CLERK
67	HARRISON B. INGRAM	10/10/68	OFFICE ASSISTANT
68	IDUNNA C. JONES	10/10/68	RECEPTIONIST
69	JACOB D. KEENE	10/10/68	FILE CLERK
70	KENNETH E. LAURENCE	10/10/68	TRAINING OFFICER
71	LUCILLE F. MANN	10/10/68	LABORATORY ASST.
72	MARTIN G. NORMAN	10/10/68	INVESTIGATIVE DIVISION
73	NANCY H. OWENS	10/10/68	CHIEF OF POLICE
74	OSCAR I. PERDUE	10/10/68	CLERICAL SUPPORT
75	PATRICK J. RILEY	10/10/68	LABORATORY
76	QUENTIN K. SCHMIDT	10/10/68	RECORDS & COMMUNICATIONS
77	ROSAMUND L. SIMPSON	10/10/68	ADMINISTRATIVE SERVICES
78	SCOTT M. STONE	10/10/68	CLERICAL SUPPORT
79	TERRA N. TAYLOR	10/10/68	TRAINING DIVISION
80	UDYNN O. THOMAS	10/10/68	PROPERTY CLERK
81	VANCE P. TORRES	10/10/68	OFFICE ASSISTANT
82	VERNON Q. TURNER	10/10/68	RECEPTIONIST
83	WILLIAM R. VAUGHN	10/10/68	FILE CLERK
84	XENIA S. WEBSTER	10/10/68	TRAINING OFFICER
85	YVES T. WHITE	10/10/68	LABORATORY ASST.
86	ZACHARIAH U. BLACK	10/10/68	INVESTIGATIVE

WT

ROLE

WT

ROLE

WT